Available online at www.sciencedirect.com
SCIENCE DIRECT
ELSEVIER
Palaeogeography, Palaeoclimatology, Palaeoecology 237 (2006) 483–507
PALAEO
www.elsevier.com/locate/palaeo

A 164 ka record of environmental change in the American Southwest from a Carlsbad Cavern speleothem

George A. Brook [a,*], Brooks B. Ellwood [b], L. Bruce Railsback [c], James B. Cowart [d]

[a] Department of Geography, University of Georgia, Athens, GA 30602, United States
[b] Department of Geology and Geophysics, Louisiana State University, Baton, Rouge, LA 70803, United States
[c] Department of Geology, University of Georgia, Athens, GA 30602, United States
[d] Department of Geology, Florida State University, Tallahassee, FL 32306, United States

Received 14 January 2005; received in revised form 2 December 2005; accepted 7 January 2006

Abstract

A horizontal core 2.8 m in length drilled from the Georgia Giant column in Carlsbad Cavern provides climate information for the last 164 ka. Forty-six alpha spectrometric U-series ages determined at intervals of ~7.6 cm along the core indicate five periods of deposition and five hiatuses, the longest from 136 to 110 ka. Variations in growth rate (0 to 70 mm/ka), in the abundance of aragonite, chalcedony, and Fe-bearing phases, and in ^{13}C indicate that glacial intervals of the last 164 ka, OIS 6, 4, and 2, were much wetter than today, as were the colder substages 5d and 5b of OIS 5. By contrast, during the two warmest periods of the past 164 ka, namely OIS 5e and 1, there was no deposition on either side of the speleothem, suggesting conditions as dry or drier than today.

The record from Carlsbad parallels data from many other sites in the southwestern USA and northern Mexico, and data from marine sediments and ice cores, demonstrating the extent to which ice sheet fluctuations influenced conditions in southern New Mexico. Detailed correlation of $\delta^{13}C$ values in the Georgia Giant, which range from −6.6 to +0.9‰ relative to PDB, with distant speleothem records and with data from ice cores, further documents the linkage of southwestern climate with global-scale extent of glaciation.

Values of $\delta^{18}O$ in the Georgia Giant core range from −9.7 to −4.7‰ relative to PDB and average −6.6‰. ^{18}O-depleted carbonate in the Georgia Giant during OIS 6, at a time when the world's oceans were enriched in ^{18}O, suggests that precipitation during cold intervals was brought largely by Pacific air masses in fall, winter and spring as a result of the southward displacement of the polar jet stream by the growth of the Laurentide Ice Sheet.

Termination II, marking the end of the penultimate glaciation, is well defined in the core's $\delta^{18}O$ data. Analytical uncertainties in the radiometric ages do not preclude a start of Termination II as late as 128 ka, as suggested by SPECMAP data. However, data from the Georgia Giant core are more compatible with an earlier start like that obtained from Devils Hole and Vostok data, raising the possibility that early warming was widespread in the U.S. southwest region by 145 ka.

1. Introduction

Secondary carbonates have provided important records of environmental change in the western United States (Winograd et al., 1988; Szabo, 1990; Winograd et

* Corresponding author. Tel.: +1 706 542 2322; fax: +1 706 542 2388.
E-mail address: gabrook@uga.edu (G.A. Brook).

0031-0182/$ - see front matter © 2006 Elsevier B.V. All rights reserved.
doi:10.1016/j.palaeo.2006.01.001

al., 1992; Szabo et al., 1994). For example, stable isotope studies of carbonate at Devils Hole, Nevada, have revealed systematic changes in air temperature and/or air mass characteristics from 565 to 60 ka, with interglacials relatively warm and dry and glacials significantly cooler and wetter than now (Winograd et al., 1988, 1992). In addition, the TIMS-dated Devils Hole record has raised questions about the timing of the end of the penultimate glaciation (Termination II) relative to the SPECMAP ocean core chronology based on solar insolation peaks at high latitude (e.g., Imbrie et al., 1984; Martinson et al., 1987; Edwards and Gallup, 1993; Crowley, 1994). However, thus far the Devils Hole record provides no data after 60 ka and so cannot be used to assess conditions during oxygen isotope stages (OIS) 3, 2 and 1.

Earlier studies have shown that stalagmites in Carlsbad Cavern, New Mexico, preserve a record of past conditions (e.g., Brook et al., 1990; Polyak and Asmerom, 2001; Polyak et al., 2004), and large speleothems in the cave probably contain long records of conditions in southeastern New Mexico over many hundreds of thousands of years. In this paper we report on a horizontal core 2.8 m long that was drilled from a large Carlsbad column, the Georgia Giant, in the Green Lake Room, in order to extract one such long paleoenvironmental record extending to the most recent oxygen isotope stages.

2. Carlsbad Cavern

Carlsbad Cavern within Carlsbad Caverns National Park is in the Guadalupe Mountains of southeastern New Mexico in the northeastern Chihuahuan Desert (Fig. 1). The extensive cave system has developed in the Permian Capitan Reef complex. It consists of elongated passages and wide rooms trending NNW to ENE that extend to a depth of almost 300 m beneath the natural cave entrance at an elevation of 1325 m amsl and 180 m below the floor of Walnut Canyon ~2 km to the north. Passages have formed in four Upper Permian stratigraphic formations, the Tansill, Yates, Seven Rivers, and Capitan Limestone (Gonzalez and Lohmann, 1988). Mean annual precipitation is 379 mm, with ~80% falling in 6 months, from May through October. Snowfall averages ~14 cm/year. Mean annual, winter, and summer air temperatures are 16.9 °C, 8 °C, and 25 °C (Western Regional Climate Center, wrcc@dri.edu).

Current vegetation includes cactus, succulents, and desert shrubs in the lower Guadalupe Mountains, transitional to montane coniferous forest on the upper Guadalupe ridges. Past climate was moister and cooler than today and during much of the Pleistocene pinyon–juniper–oak forests reached lower elevations (e.g., Van Devender, 1990; Betancourt et al., 2001). Williams (1983) notes that soils on the surface of the upland above the cave are absent, very thin, or confined to widened joints. Most of the surface consists of rocky outcrops of solutionally pitted dolomitic rocks irregularly covered with low scrub and cactus vegetation.

The regional groundwater table at Carlsbad Cavern is ~30 m below the deepest passages (Hill, 1987) so that the only water entering the cave percolates in from the surface. Although drip rates vary seasonally, being highest in September–October (McLean, 1976), the time lag of the pressure pulse between storm events and drip activity (e.g., 2–5 weeks for a drip at Green Lake) indicates considerable storage of water in an upper weathered layer of rock (the subcutaneous zone) at the top of the vadose zone (Williams, 1983). Stable isotope characteristics and tritium activity of drip and pool waters indicate 17–36 year travel times through the vadose zone to the main cave level ~209 m below the entrance (Ingraham et al., 1990; Chapman et al., 1992). These slow percolation rates, and the lack of a significant pressure pulse on drips after rainfall, suggest a capillary barrier at the base of the subcutaneous zone (Williams, 1983). This "bottleneck" regulates percolation to deeper parts of the aquifer, and to Carlsbad Cavern.

The climate of Carlsbad Cavern, CO_2 content of the cave air, and to some extent the $\delta^{18}O$ and $\delta^{13}C$ of drip and pool water are modulated by outside air temperature. Temperature in the cave ranges from 13.5 to 15.5 °C, and relative humidity from 86% in open, dry rooms to 100% in closed rooms and constricted passages (Gonzalez and Lohmann, 1988). Lower temperature, relative humidity and pCO_2 and higher evaporation in winter than in summer are due to pulses of dense, cold, dry air that sink into the natural entrance of the cave when the outside air temperature drops below 14 °C, the average temperature in the cave (McLean, 1971). In addition, the cave reportedly "breathes out" during stormy weather associated with falling air pressure and "inhales" during dry, fair weather when air pressure is high (Boyer, 1964). This "breathing" must periodically reduce pCO_2 and humidity in the cave.

In February 1995 the volume of Green Lake (250 m below the surface) in the Green Lake Room near the Georgia Giant, was calculated as 44 m^3 based on dilution of a bromide tracer (Forbes, 2000). Although this relatively large body of water moderates temperature

Fig. 1. Location map showing Carlsbad Cavern and other important sites mentioned in the text.

and increases average humidity in this part of the cave, seasonal influences are still apparent. For instance, in August and October 1994 air temperatures were slightly warmer (13.9 °C and 14.2 °C) than in January and April 1995 (13.6 °C, and 13.9 °C), and relative humidity higher (97 and 97% compared to 88 and 92%). Also, the inflow of dry winter air and reduced outgassing of CO_2 due to slower drip rates saw air CO_2 drop from 1000 ppm in October 1994 to 330 ppm in January 1995 (Forbes, 2000). Cave air pCO_2 appears to reach maximum levels around October due to stable air conditions in the cave and increased CO_2 outgassing due to higher drip rates following the rainy season. In October 1985, for example, CO_2 at various points in the cave varied from 450±50 to 1000±50 ppm (Hill, 1987) while Forbes (2000) reports levels five times atmospheric in some passages.

Normally, monthly PET at the cave is higher than precipitation for all months of the year; however, due to the thin soil cover and sparse vegetation infiltration to the cave occurs during infrequent, irregular periods of high rainfall in both summer and winter (McLean, 1971). The narrow $\delta^{18}O$ range for drips at many depths and locations in Carlsbad (e.g., Ingraham et al., 1990; Chapman et al., 1992) indicates that infiltrating precipitation events are well mixed in the subcutaneous zone before they penetrate the deeper parts of the aquifer and enter the cave. With decadal flow-through times, observed seasonal changes in the isotopic composition of drip water, with slight enrichment in ^{18}O in late fall, winter and spring, may be due to seasonal changes in cave microclimate, rather than seasonal changes in the isotopic composition of rainfall. Cold dry conditions in winter may lead to some evaporation of water in the

Table 1
Monthly precipitation and temperature, Carlsbad Cavern

	Jan	Feb	Mar	Apr	May	Jun	Jul	Aug	Sept	Oct	Nov	Dec	Year
Temperature (°C)	7.2	9.2	12.4	16.9	21.3	25.2	25.8	25.1	22.0	17.5	11.7	8.0	16.9
Precipitation (mm)	12	11	9	16	38	45	50	60	76	36	12	13	379
Snowfall (mm)	33	28	18	2	0	0	0	0	0	2	10	46	137

Period of record: 2/1/1930–7/31/2000; source: Western Regional Climate Center, wrcc@dri.edu.

bedrock before it drips into the cave and also to exchange with ^{18}O-depleted vapor in the cave air (Ingraham et al., 1990; Chapman et al., 1992: Forbes, 2000). However, longer-term variations in the relative amount of summer infiltration are discernible in the isotopic composition of the drip water in the cave (Chapman et al., 1992). Increased drip rates may limit the effect of the cave microclimate on water chemistry and isotopic characteristics. After heavy rains in 1984, 15% of seepage waters collected in August and September were undersaturated with respect to calcite and aragonite while in May 1985 all were saturated (Gonzalez and Lohmann, 1988). Reduced outgassing of CO_2 and less evaporation in the bedrock above the cave may explain this change in water chemistry (Table 1).

3. Methodology

A 2.8 m, 5 cm-diameter, horizontal core 2.8 m in length and 5 cm in diameter was drilled through the Georgia Giant column in the Green Lake Room, 215 m below the natural cave entrance and 120 m below the floor of Walnut Canyon ~2 km to the north (Fig. 2). The outer 5 to 7.5 cm of the column at either end of the core was weathered and fragmented when drilled and could not be retained. We report our results relative to distance along the core from the side of the column on which the drill first penetrated.

Smaller cores 2.4 cm in diameter were drilled from the larger core segments and were cut into 105 pieces 2.2 cm in length. Remanent magnetism (RM) was measured on these smaller cores using the SCT cryogenic magnetometer at the University of Pittsburgh. Stepwise a.f. demagnetization was performed at 5 mT at 10 mT steps to 50 mT on all samples with a natural RM greater than 4×10^{-5} A/m. Several core samples were also given an isothermal remanent magnetism (IRM) at 20, 40, 60, 80, and 100 mT. Magnetic susceptibility (MS) was also measured on these core sections.

Forty-six alpha spectrometric U-series (AS) ages at intervals of ~7.6 cm provided a chronology for the core (Table 2, Fig. 3). The samples utilized for dating were exceptionally free of non-carbonate inclusions; dissolution of the samples revealed either non-observable or very minimal detritus. The carbonate also appeared exceptionally pure in thin section when compared with numerous speleothem samples that we have examined (e.g., Railsback, 2000). In almost all of the samples analyzed, the ^{232}Th peak was indiscernible even with a very low background. However, ^{230}Th/^{232}Th ratios were calculated for 6 samples with perceptible ^{232}Th spectral peaks. Values varied from 42±14 for G116 to 2229±866 for G72 (G6=277±100, G9=276±140, G75=479±108, G81=601±208, G84=291±49, G87=427±187) indicating extremely low ^{232}Th even in samples with discernible ^{232}Th peaks. For this reason ^{230}Th/^{232}Th ratios were not estimated for most samples and no correction for "contaminant" ^{230}Th was applied in any of the sample age calculations.

δ^{18}O and δ^{13}C values were measured at intervals of ~2.5 cm along the core, and at smaller intervals to provide more detail in areas of rapid change. Carbon

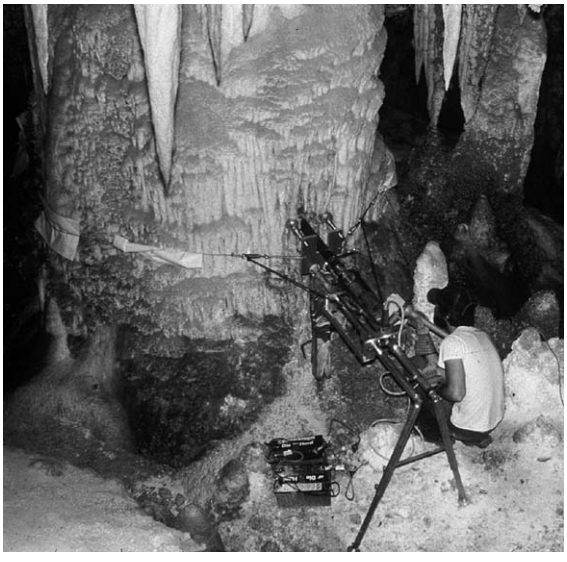

Fig. 2. Drilling the 2.8 m-long core from the Georgia Giant (photograph by Brooks B. Ellwood).

Table 2
Uranium-series age data and Fe-bearing layers, Georgia Giant core

Sample ID	Distance along core (cm)	Uranium concentration (ppm)	$^{234}U/^{238}U$ activity ratio	Initial $^{234}U/^{238}U$ activity ratio	$^{230}Th/^{234}U$ activity ratio	Age ka ($\pm 2\sigma$)
Fe-rich layer at 10 cm, 0.4 cm wide						
G6	14.7	2.46±0.07	2.55±0.07	3.00±0.07	.508±0.030	71.0±5.5
Fe-bearing layer at 19.5 cm, 0.2 cm wide						
G9	22.3	0.89±0.03	2.55±0.07	3.09±0.08	.565±0.042	81.8±8.5
G12	29.9	1.34±0.03	2.55±0.04	3.17±0.05	.607±0.017	90.5±3.8
Fe-bearing layer at 32.2 cm, 0.2–0.3 cm wide						
G14	37.0	0.90±0.03	2.47±0.07	3.10±0.09	.649±0.024	99.9±5.6
Fe-bearing layer at 37.5 cm, 0.5 cm wide						
G16	40.4	0.45±0.01	2.48±0.06	3.26±0.08	.728±0.021	119.0±5.7
G18	45.0	0.48±0.01	2.42±0.05	3.30±0.07	.788±0.020	135.8±6.1
G20	50.7	0.50±0.01	2.28±0.05	3.10±0.07	.793±0.037	138.2±11.5
G21	52.7	0.62±0.02	2.28±0.08	3.22±0.11	.836±0.039	151.7±13.7
G24	60.2	0.49±0.02	2.30±0.10	3.10±0.13	.779±0.039	133.8±12.0
G27	67.9	0.40±0.01	2.32±0.06	3.23±0.08	.823±0.027	147.0±9.0
G30	75.5	0.40±0.01	2.27±0.06	3.14±0.08	.818±0.026	146.1±8.5
G33	83.2	0.48±0.01	2.22±0.06	3.09±0.08	.827±0.024	149.2±8.3
G36	90.7	0.37±0.01	2.26±0.08	3.14±0.11	.828±0.062	149.4±20.8
G39	98.3	0.39±0.01	2.19±0.06	3.16±0.09	.877±0.028	167.0±11.1
G41	103.4	0.39±0.01	2.20±0.07	3.03±0.10	.820±0.028	147.3±9.6
G42	105.8	0.37±0.02	2.17±0.16	2.95±0.22	.809±0.056	144.0±18.7
G45	113.5	0.34±0.01	2.20±0.07	3.23±0.10	.896±0.030	174.1±12.3
G48	121.2	0.38±0.03	2.22±0.07	3.18±0.10	.861±0.029	160.6±11.0
G50[a]	127.5	0.64±0.02	1.89±0.06	2.37±0.09	.824±0.042	153.3±15.0
G51	128.8	0.38±0.01	2.16±0.07	2.93±0.09	.799±0.032	140.8±10.4
G54	136.4	0.48±0.01	2.16±0.06	3.00±0.09	.837±0.033	153.2±11.7
G57	144.0	0.49±0.01	2.19±0.06	3.02±0.08	.820±0.030	147.2±10.0
G60	151.7	0.44±0.01	2.20±0.07	3.05±0.08	.826±0.026	149.2±9.1
Fe-bearing layers at 157 and 158.2 cm, 0.1–0.2 and <0.1 cm wide respectively						
G63	159.3	1.89±0.04	2.23±0.04	3.04±0.05	.803±0.025	141.7±8.1
Fe-bearing layers at 162.2 and 163.1 cm, each <0.1 cm wide						
G65	164.8	0.87±0.03	2.51±0.09	3.22±0.11	.681±0.025	107.0±6.1
G66	166.9	3.08±0.09	2.46±0.04	3.19±0.05	.708±0.019	113.9±4.9
G69	174.5	0.79±0.02	2.55±0.05	3.27±0.06	.678±0.020	106.3±4.9
Fe-bearing layer at 176 cm, 0.2–0.7 cm wide						
G72	182.0	0.89±0.02	2.51±05	3.19±06	.663±0.021	102.8±5.0
Fe-bearing layer at 188 cm, 0.4 cm wide						
G75	189.6	1.36±0.05	2.54±0.06	3.13±0.07	.609±0.019	90.9±4.1
G76[a]	190.8	1.61±0.03	1.61±0.03	2.63±0.03	.615±0.024	93.2±5.3
Fe-bearing layer at 192.8 cm, 0.3–0.7 cm wide						
G78	197.2	1.80±0.10	2.63±0.08	3.25±0.10	.609±0.026	90.6±5.6
G81	204.8	3.57±0.17	2.67±0.04	3.24±0.06	.571±0.029	82.9±5.9
Fe-bearing layers at 210.3 and 210.8 cm, each <0.1 cm wide						
G84	212.3	2.42±0.19	2.62±0.05	3.25±0.06	.610±0.027	90.8±5.8
Fe-bearing layers at 212.5, 213.5 and 213.7 cm, each <0.1 cm wide						
G87	220.0	1.31±0.12	2.74±0.08	3.18±0.09	.469±0.026	63.7±4.5
G90	227.6	2.81±0.15	2.79±0.05	3.29±0.06	.497±0.021	68.7±3.9

(continued on next page)

Table 2 (*continued*)

Sample ID	Distance along core (cm)	Uranium concentration (ppm)	$^{234}U/^{238}U$ activity ratio	Initial $^{234}U/^{238}U$ activity ratio	$^{230}Th/^{234}U$ activity ratio	Age ka ($\pm 2\sigma$)
Fe-bearing layers at 212.5, 213.5 and 213.7 cm, each <0.1 cm wide						
G93	235.2	0.91±0.04	2.78±0.10	3.20±0.11	.447±0.016	60.0±2.8
Fe-bearing layers at 237.9, 238.4, 238.8 and 239.5 cm, each <0.1 cm wide						
G96	242.9	0.75±0.02	3.00±0.08	3.51±0.09	.466±0.022	63.1±2.2
G99	250.3	1.60±0.05	2.89±0.05	3.32±0.06	.431±0.015	57.3±2.5
Fe-bearing layers at 255.8, 256.1 and 256.5 cm, each <0.1 cm wide						
G102	258.0	0.77±0.02	2.77±0.06	3.12±0.07	.388±0.027	50.4±4.2
G105	265.5	0.61±0.02	2.87±0.07	3.23±0.08	.373±0.015	48.1±2.3
G108	273.2	0.62±0.02	2.91±0.07	3.22±0.08	.335±0.017	42.3±2.5
G109[a]	278.3	0.45±0.04	2.82±0.26	3.06±0.29	.347±0.030	44.1±4.5
G110	278.5	0.68±0.02	2.98±0.08	3.32±0.09	.343±0.009	43.4±1.3
G113	287.0	0.69±0.03	2.84±0.11	3.10±0.12	.300±0.019	37.2±2.7
G114[a]	288.4	0.63±0.02	2.99±0.10	3.14±0.10	.210±0.008	25.0±1.0
Fe-bearing layer at 289.0 cm, <0.1 cm wide						
G116	293.7	0.47±0.02	2.88±0.11	3.00±0.11	.154±0.014	17.9±1.7
G119[a]	301.1	0.37±0.01	2.94±0.10	3.00±0.10	.102±0.005	11.6±0.6
G122	309.9	0.48±0.02	2.89±0.14	3.00±0.14	.126±0.013	14.4±1.5
G124	315.0	0.63±0.01	2.92±0.05	3.00±0.05	.105±0.003	12.0±0.4
G125	317.5	0.63±0.03	2.86±0.15	2.94±0.15	.102±0.011	11.5±1.3

[a] Kathleen Cole obtained these ages while a staff member of the Center for Applied Isotope Studies, University of Georgia.

dioxide was generated from 12 to 20 mg of powdered carbonate by reaction with phosphoric acid (H_3PO_4) according to procedures described in McCrea (1950). Relative isotopic abundances in the liberated CO_2 were determined with a V. G. Micromass 602c mass spectrometer. Replicate analyses indicate a reproducibility of ±0.2l. As oxygen and carbon are fractionated differently when deposited as aragonite compared to coprecipitated calcite (aragonite has higher isotopic values than calcite) all values of $\delta^{18}O$ and $\delta^{13}C$ for drilled samples containing aragonite were corrected to equivalent calcite values. This entailed subtracting 1.7‰ from the carbon values (Romanek et al., 1992) and 1.0‰ from the oxygen values (Grossman and Ku, 1986) of samples composed of 100% aragonite and subtracting a proportion of this from samples consisting of both calcite and aragonite. The percentage of aragonite was estimated by examining thin sections and by visual inspection of the core near the drill hole. Four drilled samples (at 32.3, 37.5, 38.2 and 210.5 cm) were 100% aragonite. Eight other samples from 212.2, 216.2, 238.2, 281.2, 287.5, 287.8, 289.5 and 290.0 cm contained 50%, 30%, 80%, 5%, 10%, 10%, 20%, and 20% aragonite, respectively. All drilled samples with 10% or more aragonite were adjacent to prominent Fe-bearing layers. We believe that our estimates of aragonite content have a maximum uncertainty of ±20%. So, samples with an estimated 100% aragonite have $\delta^{18}O$ uncertainties of +0.2‰ and −0.4‰ and $\delta^{13}C$ uncertainties of +0.2‰ and −0.54‰ if mass spectrometer reproducibility (±0.2‰) and aragonite uncertainties (+0.0 and −0.2‰ for oxygen and +0.0 and −0.34‰ for carbon) are added. By similar reasoning, samples with 50%, 20%, 10% and 5% aragonite will have $\delta^{18}O$ uncertainties of ±0.4‰, ±0.4‰, −0.4‰/+0.3‰, and −0.4‰/+0.25‰, respectively, and $\delta^{13}C$ uncertainties will be ±0.54‰, ±0.54‰, −0.54/+0.37‰, and −0.54/+0.28‰, respectively. In Figs. 3 and 5, these uncertainties are contained within the symbols for the data points.

According to Hendy (1971), if the $\delta^{18}O$ of speleothem carbonate is constant along a growth layer, and there is no correlation between the $\delta^{18}O$ and $\delta^{13}C$ this indicates that deposition was in equilibrium with precipitating waters. “Hendy” tests were not conducted on the Georgia Giant core because: (i) we could only sample extremely small sections (4–9 cm) of growth layers in the ~6 m high column, (ii) there were few visible growth layers in the core and these were mostly in areas with higher aragonite on the steeply dipping flanks of the deposit where kinetic fractionation would be more likely, (iii) isotopic values from samples drilled in areas of both aragonite and calcite (oxygen and carbon are fractionated differently—see above) would be difficult to interpret if the exact content of aragonite in the drilled sample was not known, and

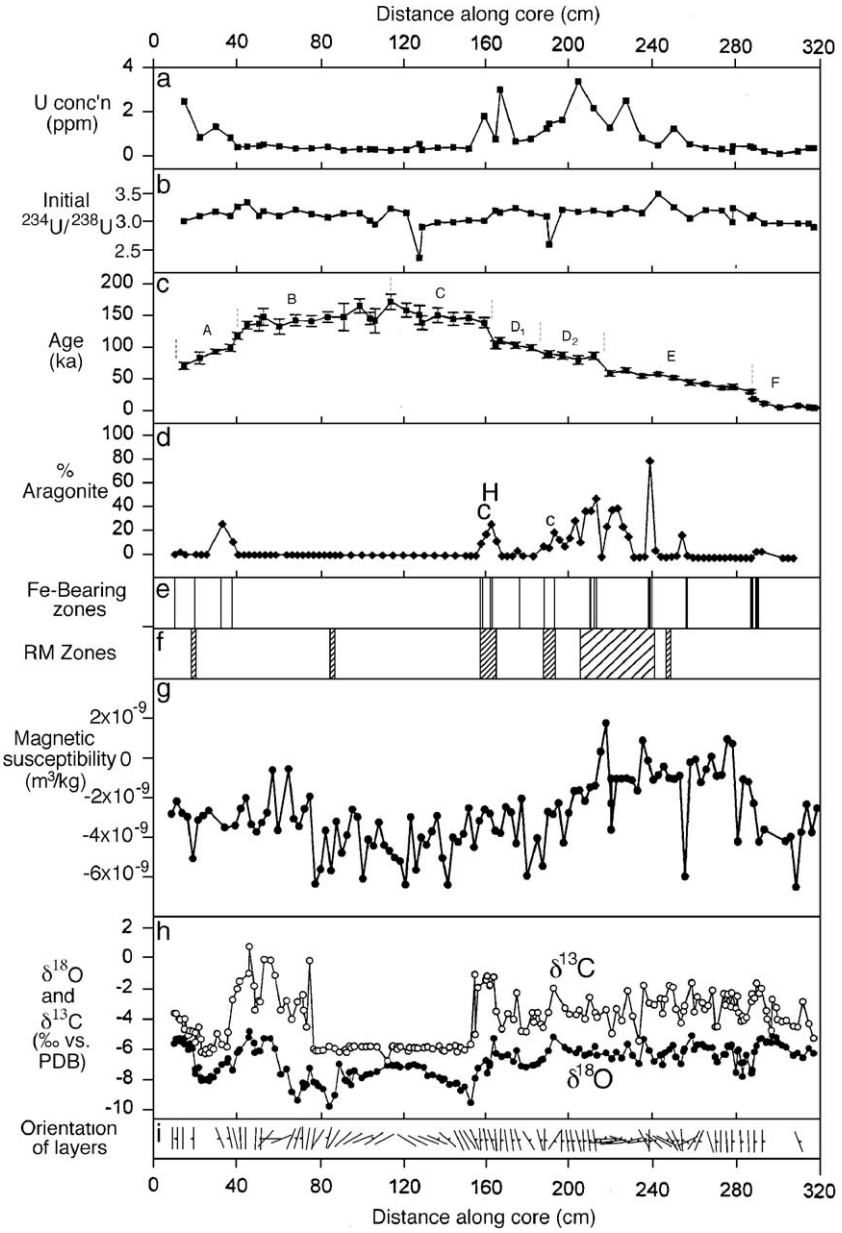

Fig. 3. Variations along the Georgia Giant core. (a) and (b) U concentrations and initial $^{234}U/^{238}U$ ratios. (c) AS ages (squares) and uncertainties (bars). Letters label intervals across which linear regression is shown in Fig. 4. (d) Abundance of aragonite as determined petrographically by scanning thin sections. "C" indicates layers of chalcedony; "H" indicates petrographically distinct hiatus. (e) Fe-bearing zones as recognized petrographically. (f) Zones with measurable remanent magnetism. (g) Magnetic susceptibility. (h) $\delta^{18}O$ and $\delta^{13}C$ of speleothem carbonate. Isotopic values for twelve drilled samples consisting of 5–100% aragonite were corrected to 100% calcite equivalents. Aragonite was determined for the area of the drill hole from thin sections by visual examination. (i) Orientation of layers. Small appendages indicate direction of growth as recognized petrographically.

(iv) some of the visible partings in the core mark periods of slow or no deposition and so are not suitable for equilibrium tests. Significantly, there were no visible growth lines in the central part of the core where crystal orientations indicate horizontal layering at the top of a growing stalagmite.

4. Core characteristics

4.1. Stratigraphy and mineralogy

Layering in the Georgia Giant core can be recognized at boundaries between different minerals, and growth

directions can be inferred from orientations of aragonite botryoids and from terminations of calcite crystals. Layers are nearly vertical at the beginning of the core (e.g., 10 to 53 cm), but their dip lessens to horizontal at 119 cm before increasing again to steep dips from 163 to 315 cm (with a minor near-horizontal area from 216 to 234 cm) (Fig. 3). The horizontal zone at 119 cm coincides with the zone of greatest radiometric age at 114 to 122 cm. The center of the speleothem is thus at 119 cm in terms of growth history and morphology. The small zone of horizontal layers from 216 to 234 cm may reflect composite growth of a secondary column, now overgrown, on the distal side of the speleothem around 50 ka.

The core consists almost entirely of calcite and aragonite, but they are not distributed uniformly. Large portions of the core (e.g., from 41 to 155 cm) consist entirely of calcite. Other sections (e.g., 155 to 258 cm) are up to 81% aragonite (Fig. 3). Calcite is generally more abundant in intervals where layers are nearly horizontal (e.g., 100 to 142 cm), whereas aragonite is more abundant where layers dip steeply (e.g., 192 to 219 cm). However, that relationship is far from universal, in that some nearly horizontal intervals have significant proportions of aragonite (e.g., 220 to 240 cm) and some steeply dipping intervals are entirely calcite (e.g., 260 to 287 cm) (Fig. 3).

Calcite in the core is largely columnar to palisade calcite (as defined by Railsback, 2000). Individual calcite crystals are as much as 17 mm long, and they are commonly devoid of any inclusions. Aragonite is present as botryoids in which individual crystals are 0.012 mm to 2.65 mm long. Some aragonite botryoids have calcite within them, suggesting that some aragonite has partially recrystallized to calcite. Uranium concentrations range from 0.34 to 3.54 ppm (Fig. 3) and are largely a function of the percentage of aragonite: aragonite-rich intervals (e.g., 158 to 240 cm) typically have higher U concentrations than those in calcite-rich intervals (e.g., 41 to 155 cm), which is in accord with the higher distribution coefficient of U in aragonite relative to that in calcite (Kitano and Oomori, 1971; Meece and Benninger, 1993).

The core was almost entirely white when first taken, but thin pale tan to orange-red zones appeared shortly after the core was cut and sub-sampled. We interpret this color change to be the result of oxidation of Fe-bearing compounds such as siderite ($FeCO_3$) or ankerite to very fine-grained maghemite/hematite (Ellwood et al., 1986, 1989), as the core was exposed to oxygen. These tan to orange-red zones are commonly associated with aragonite layers. Examination via scanning electron microscopy (SEM) shows that aragonite in such zones is associated with, and at least locally coated with, smectite. Energy dispersive analysis (EDS) confirms that the chemical composition of the smectite is Mg–Si–O, and the morphology of the smectite suggests an authigenic rather than detrital origin. EDS yields no evidence of Fe in these zones, suggesting that only a small concentration of Fe accounts for the pale tan to orange-red color observed after oxidation. Such zones are found at 10, 19.5, 32.2, 37.5, 157 to 163.1 (four thin layers), 176, 188, 192.8, 210.6–210.8 (two thin layers), 212.5–213.7 (three thin layers), 237.9–239.5 (four thin layers), 255.8–256.5 (three thin layers), and 286.8–290.6 cm (seven thin layers) (Fig. 3, Table 2).

Layer relationships at 164.1 cm suggest a major hiatus in speleothem growth. Here, layers of aragonite underlie and overlie an Fe-rich zone similar to the pale tan to orange-red smectitic zones discussed above. Overlying the most recent aragonite layer is a calcite layer that recurves over the aragonite. Calcite crystals have grown downward onto the pre-existing aragonite. This relationship suggests a hiatus at which the aragonite layer was exposed for a considerable time. An abrupt decrease in U-series age from 135 ka to 100 ka (Figs. 3c, 4a, b; Table 2) across this zone confirms this petrographically identified hiatus. The core's most prominent occurrence of chalcedony is at 163 cm, where it is present as a layer 0.04 mm thick that was deposited shortly before the hiatus at 164 cm. Four Fe-rich layers are present in the 7 cm below the hiatus at 164 cm.

4.2. Chronology and growth rates

AS ages increase from 71.0±5.6 ka at 14.7 cm to 174.0±12.3 ka at 113.5 cm along the core and then decrease to 11.5±1.3 ka at 317.5 cm (Fig. 3c). These ages indicate seven periods of continuous growth separated by times of slow or no growth. However, large 2σ errors have resulted in age reversals in some sections of the core, making it difficult to apply ages to other core data such as stable isotope values. To overcome this problem, steady growth was assumed during each of the seven phases of deposition, and linear regression was used to assign ages within each phase (Fig. 4). Regression lines pass through the 2σ error bars of most samples and suggest that the oldest part of the core (~164 ka) is at 113–114 cm (Fig. 3). The most pronounced discontinuity in the series of ages, and thus the greatest hiatus, is at 164 cm along the core and between 130 and 105 ka.

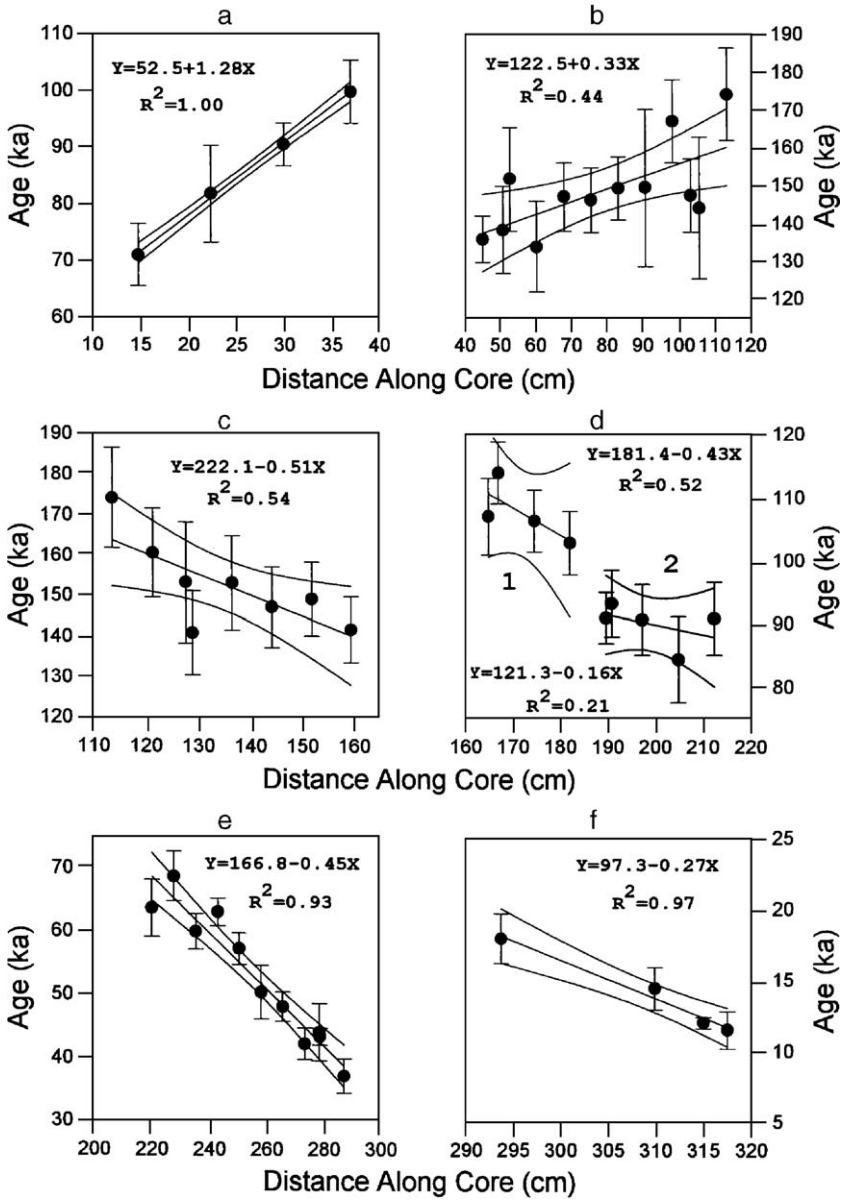

Fig. 4. Age-distance regressions for intervals of the Georgia Giant core. Intervals used are also shown in Fig. 3c.

Inversion of the slopes in Fig. 4 yields apparent growth rates. Correction to account for the dip of the speleothem's layers requires conversion by the equation

$$\mathrm{Rate}_{\mathrm{true}} = \mathrm{Rate}_{\mathrm{apparent}} \times \sin(\mathrm{dip}).$$

Application of this equation to either side yields growth rates varying from 0 to 63 mm/ka. Our data show that at times there was growth on only one of the two sides of the column sampled by our core and at other times on both. By adding growth rates on the two sides we were able to obtain a reasonable record of variations in the growth of the column over time, with total rates ranging from 0 to 70 mm/ka (Table 3).

4.3. Magnetic properties

Magnetizable materials in cave sediments include not only the ferrimagnetic minerals that may acquire remanent magnetism (RM), but also any other compound containing Fe^{2+}, Fe^{3+}, or Mn^{2+} ions and compounds with odd numbers of electrons. These less magnetic, (paramagnetic) substances include clay minerals, particularly chlorite, smectite, illite and

Table 3
Ages of Fe-bearing layers, Georgia Giant core

Depth (cm)	Age (ka)	OIS[a]
286.8, 287.0, 287.7,289.0, 289.3, 290.0, 290.6	38–37	3
255.8, 256.1, 256.5	52	3
239.5, 238.8, 238.4, 237.9	60	4/3
19.5	78	5a
210.6, 210.8, 212.5, 213.5, 213.7	88–87	5b
188.0, 192.8, 32.2[b]	95–91	5b
176.0, 37.5[b]	105–102	5c
162.2, 163.1, 157.0, 158.2	142–139	6/5

[a] With reference to the marine SPECMAP record of Imbrie et al. (1984) and Martinson et al. (1987) and our $\delta^{18}O$ and $\delta^{13}C$ data for the Georgia Giant.
[b] Layers on both sides of the speleothem.

glauconite; ferromagnesian silicates; iron and manganese carbonates; iron sulfides like pyrite and marcasite; and authigenic ferric-oxyhydroxides. Calcite, on the other hand, is diamagnetic, acquiring a negative magnetization within an inducing magnetic field.

The Georgia Giant core yielded 21 samples with an initial RM intensity great enough to measure effectively (Fig. 3), indicating the presence of a ferromagnetic component, probably either magnetite or maghemite. Many of these samples show an RM characterized by linear decay to the origin of demagnetization paths, although less ideal behavior is also present. Isothermal remanent magnetism (IRM) data for samples from the Georgia Giant were compared with IRM data for fine-grained magnetite (~0.5 μ) and hematite (~0.5 μ) synthetic samples. The Georgia Giant samples are intermediate between the two standards suggesting a mixture of magnetite and hematite in the carbonate of the core.

RM directions for the 21 samples exhibiting reasonable demagnetization behavior (general straight-line to the origin decay) are generally well clustered with only a few exceptions. The mean RM direction for 15 samples from this data set is $D=341.9°$, with $I=43.3°$, after exclusion of samples with apparently anomalous declinations or inclinations. These values are approximately 18° and 8.5°, respectively, less than the axially centered geomagnetic field direction.

Magnetic susceptibility (MS) of core samples was also measured. MS (X) is defined as the ratio of the induced moment (M_i) to the strength of an applied, very low-intensity magnetic field (H_j), where:

$$M_i = X_{ijb} \cdot H_j$$

When reporting MS, it is normally assumed that the measurement is relative to a given volume that is dimensionless (see the discussion by Ellwood et al., 1988). Here, we report MS in terms of sample mass because it is much easier to calculate MS with high precision, and mass MS can be directly tied to values for standards reported by the U.S. National Bureau of Standards (Swartzendruber, 1992). Volume is much more difficult to measure with high precision (Ellwood et al., 1988). The measured anisotropy of MS is negligible in these mainly diamagnetic samples and therefore has little effect on bulk MS measurement.

The distribution of samples with measurable RM correlates strongly with zones of increased aragonite in the core, periods of slow growth, Fe-bearing zones, and also with regions of relatively high $\delta^{18}O$ and $\delta^{13}C$ values (Fig. 3). MS is generally low from 80 to 150 cm corresponding to the central part of the column where $\delta^{18}O$ and $\delta^{13}C$ values are also at their lowest. It is much higher from 40 to 50 cm and between 200 and 290 cm, corresponding approximately with both higher $\delta^{18}O$ and $\delta^{13}C$ values and a higher percentage of aragonite. When RM is measurable (it was not in 84 of 105 samples), and MS high, iron is more abundant than elsewhere in the core.

4.4. Stable isotopes

Values of $\delta^{18}O$ in the Georgia Giant core range from −9.7 to −4.7‰ and average −6.6‰ ($\sigma=1.1$‰) (Figs. 3 and 5). Between 70 and 160 cm values show a marked degree of symmetry around the old, central part of the core at about 120 cm. $\delta^{13}C$ values in the Georgia Giant vary from −6.6‰ to +0.9‰ PDB, and although the average is −3.8‰ ($\sigma=1.7$‰), the distribution of values is bimodal with peaks at ~−5.6 and ~−3.5‰ (Figs. 3 and 5). Away from the center of the speleothem, $\delta^{18}O$ and $\delta^{13}C$ values increase with increasing distance, fluctuating more or less in parallel. The lowest values of both $\delta^{18}O$ and $\delta^{13}C$ occur near the oldest part of the core where carbonate was deposited on the crest of a growing stalagmite or adjacent to it (Fig. 3). We believe that the gradual increase in $\delta^{18}O$ and $\delta^{13}C$ away from the oldest part of the core reflects a small but steady increase in the kinetic fractionation of O and C isotopes in the water that precipitated the carbonate. This may have resulted from the steadily increasing distance that the waters had to travel from the top of the growing stalagmite to reach the site of our drilled core. Longer flow times may have increased evaporation and given more time for CO_2 outgassing to affect the C and O isotopes in the flowing water. Changes in $\delta^{18}O$ and $\delta^{13}C$ values through the core do not, however, correspond to change

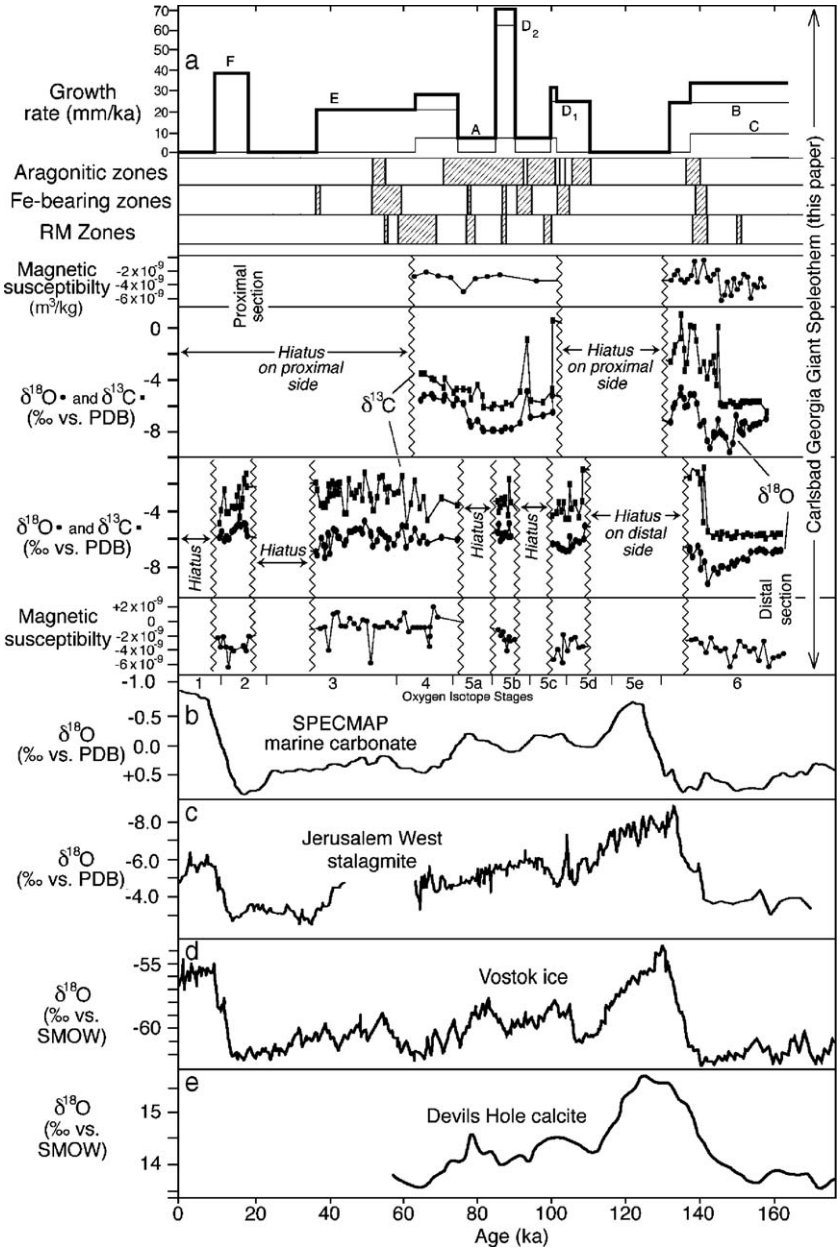

Fig. 5. The Georgia Giant record and global records. (a) Georgia Giant growth, calculated as discussed in text, and aragonitic zones, Fe-bearing zones, zones of remanent magnetism, magnetic susceptibility, and stable isotope data. Stable isotope data for samples containing aragonite are corrected to 100% calcite equivalent. For growth rate, thin lines show rates for separate sides of speleothem, so two lines are shown for intervals in which deposition occurred on both sides of the speleothem; thick line shows total. Growth rate from 88 to 92 ka is a lower-confidence calculation because of low R^2 in Fig. 4d. (b) SPECMAP marine carbonate O isotope record (Imbrie et al., 1984; Martinson et al., 1987); (c) O isotope record from Jerusalem West Cave stalagmite (Frumkin et al., 1999). This isotope record is inversely correlated to that of Carlsbad because in Israel precipitation increased during warmer climate intervals, not colder as in New Mexico. In Israel higher rainfall (more depleted in ^{18}O than lesser rainfall) and higher temperatures together led to ^{18}O depletion in the speleothem carbonate. (d) O isotope record from Vostok ice (Jouzel et al., 1987); (e) O isotope record from Devils Hole vein calcite (Winograd et al., 1992).

in dip of layers. As Figs. 3 and 5 show, there are significant variations in $\delta^{18}O$ and $\delta^{13}C$ that are superimposed on the general trend of increasing values with distance from the oldest part of the core. These changes provided paleoclimatic information for the region of the cave.

5. Interpretation

5.1. Interpretation of core characteristics

The wide ranges in petrography, growth rate, aragonite abundance, Fe abundance, and stable isotope composition in the Georgia Giant speleothem suggest considerable variation in paleoenvironmental conditions over the last 164 ka (Fig. 5). At one extreme are periods of non-deposition, most notably the interval from 130 to 110 ka centered on OIS 5e, which suggest conditions so dry that no drip water reached the speleothem. Other periods of non-deposition were from 35 to 20 ka and from 10 ka to the present.

Next in apparent dryness would be periods of deposition in which aragonite, chalcedony, and smectite formed and in which the speleothem's iron content was enriched, as is most notable from 157 to 250 cm or from 110 ka to 40 ka. Many studies have linked precipitation of aragonite to more extensive evaporation (Murray, 1954; Pobeguin, 1965; Siegel, 1965; Siegel and Dort, 1966; Thrailkill, 1971; Cabrol and Coudray, 1982), and the precipitation of smectite and chalcedony requires concentration of waters to yield supersaturation with respect to those minerals. The co-occurrence of smectite and chalcedony with aragonite in the Georgia Giant speleothem thus suggests that such zones represent periods of more extensive evaporation and may even represent minor hiatuses.

During such periods, very fine-grained oxidized Fe-bearing magnetic phases such as magnetite or maghemite in the Fe-bearing zones may have accumulated by physical settling as an aerosol. Their accumulation may have been enhanced during drier periods when inflow of cold, dry winter air may have increased and less flow of water across the speleothem did not wash them off. Lessened water supply would also have allowed more evaporation and resultant precipitation of aragonite rather than calcite, as has been observed elsewhere (Railsback et al., 1994, and references therein). An alternate and preferred hypothesis is that these Fe-bearing phases accumulated by chemical precipitation as oxygen-poor Fe^{2+}-bearing water entered the cave. O_2 contents of groundwaters in karst regions can approach zero at depths of 60 m (as demonstrated by data in McConnell et al., 1994), allowing accumulation of Fe^{2+} in solution. Maghemite or magnetite may later form from drip waters derived from such groundwater due to increased re-oxygenation during times of slower drip rates in the cave, allowing more extensive precipitation of oxidized Fe-bearing phases during drier periods. Thus either a physical or chemical mechanism of accumulation of these phases would be compatible with their deposition during periods of drier climate.

Finally, intervals of largely if not entirely calcite deposition and with growth rates in excess of 20 mm/ka appear to represent the wettest periods in the Georgia Giant record. These would include the interval from 164 to 136 ka, during OIS 6, and from 20 to 10 ka, during OIS 2. Fe-bearing zones and RM zones are also rare during these intervals (Fig. 5).

5.2. Interpretation of C isotope data

Stalagmite carbonate $\delta^{13}C$ is influenced by three broad factors (see also McDermott, 2004; Quade, 2004): (i) hydrological conditions above the cave that affect the exchange of C isotopes between meteoric waters and the bedrock; (ii) the composition and biomass of the vegetation above the cave; (iii) kinetic fractionation of carbon in precipitating waters, particularly as a result of rapid CO_2 outgassing.

Quade (2004) suggests that the longer it takes groundwater to percolate to a cave the more exchange is possible between carbon in dissolved species in the water and carbon in the limestone bedrock. As $\delta^{13}C$ of limestone is about +1‰ this leads to a gradual enrichment of dissolved species in ^{13}C. At Carlsbad Cavern increased recharge during colder, wetter glacial intervals would reduce flow-through times to the cave thereby reducing exchange of dissolved carbon with limestone bedrock, and therefore reducing enrichment of dissolved species in ^{13}C. Under drier climatic conditions residence time in the aquifer may increase leading to greater enrichment in ^{13}C.

Open-system groundwater flow conditions promote the exchange of carbon dissolved from the bedrock ($\delta^{13}C = +1‰$) with the soil air ($\delta^{13}C = -27‰$ for C_3 plants and −13‰ for C_4 plants). This minimizes enrichment of ^{13}C in dissolved species (particularly CO_3^- and HCO_3^-). Under closed-system conditions contact with soil CO_2 is quickly shut off as the water flows rapidly into the limestone. Under these conditions there is no further exchange with soil CO_2 after limestone dissolution and so dissolved species are enriched in ^{13}C relative to the open-system condition. The evidence from Carlsbad Cavern discussed above strongly suggests a well-developed subcutaneous zone in the upper part of the vadose zone above the cave with a bottleneck at its base that significantly slows percolation to deeper parts of the aquifer (Williams, 1983; Ingraham et al., 1990; Chapman et al., 1992). This being the case, we believe that solution by percolating waters is largely under open-system conditions in the

upper part of the subcutaneous zone at or above the karst water table. If water draining vertically out of the subcutaneous zone was undersaturated, there should be no bottleneck at the base of the zone. In fact, the upper passages of Carlsbad Cavern are >1 million years old (see Hill, 1987, p. 91), and it is difficult to see how undersaturated groundwaters leaving the subcutaneous zone would not have created efficient drainage routes to the cave in this time. The slow rate of percolation from the surface to the passages of Carlsbad Cavern is, in our view, strong evidence that waters are essentially saturated by the time they leave the subcutaneous zone and that saturation is achieved largely when percolating waters are at or above the karst groundwater table under conditions of open-system dissolution.

It has long been argued that the $\delta^{13}C$ of cave drip waters is significantly affected by the $\delta^{13}C$ of the CO_2 in the soil above the cave (e.g., Talma and Vogel, 1992), and that this is determined by vegetation characteristics (see Quade, 2004 for fuller discussion and references). Well-mixed air above soil has a $\delta^{13}C$ of about −6 to −8‰ (Monger et al., 1998). The $\delta^{13}C$ of soil air depends on the ^{13}C of organic matter, which is determined by the photosynthetic pathway used by plants in the vegetation cover. C_4 plants generate cellulose with a modal $\delta^{13}C$ of −13‰, but for C_3 plants the value is −27‰ (Cerling, 1984). CAM plants have values intermediate between C_3 and C_4. These isotopic values are largely transmitted to the CO_2 respired by plants and so to the CO_2 in the soil atmosphere. Cerling (1984) estimates limits of −2.2‰ and −8.5‰ for the $\delta^{13}C$ of soil CO_2 beneath pure C_4 and pure C_3 biomasses, respectively. Waters percolating through soil equilibrate with soil CO_2 and then dissolve limestone, which has a $\delta^{13}C$ of about +1‰. Under a C_3 biomass the first speleothem calcite deposited from seepage waters is likely to have a $\delta^{13}C$ of −12 to −8‰, depending on whether dissolution occurred under open- or closed-system conditions. Beneath a pure C_4 biomass, $\delta^{13}C$ of stalagmite calcite should range from −2.3 to +1.5‰, again depending on open- or closed-system hydrological conditions (Brook, 1999). Because C_3 plants are more likely to dominate at times of cool moist climate with cool-season wetness, whereas C_4 plants prefer warmer drier conditions and moisture in the warm season, $\delta^{13}C$ of speleothem carbonate has the potential to be a climate proxy.

The use of Georgia Giant carbonate $\delta^{13}C$ as a climate proxy depends partly on the vegetation history above the cave and how this would have affected $\delta^{13}C$. Packrat midden and soil carbonate isotopic records for the northern Chihuahuan Desert (Van Devender et al., 1979, 1984; Van Devender, 1990; Monger et al., 1998; Buck and Monger, 1999; Betancourt et al., 2001) provide considerable insight into possible changes since the last glacial. The midden evidence is clear that during the late Pleistocene pinyon–juniper–oak woodland (C_3) covered rocky slopes between 600 and 1700 m, while $\delta^{13}C$ values for late Pleistocene- and Holocene-age soil carbonates indicate that at the same time valley and basin floors with deep soils supported desert, C_4 grasslands (Monger et al., 1998; Buck and Monger, 1999). $\delta^{13}C$ values for Pleistocene fossil bison, mammoth, and horse tooth enamel from southern New Mexico, southern Arizona and Texas, indicate that these megaherbivores were eating mostly C_4 plants in the late Pleistocene, adding to the evidence for C_4 grasslands during this period (Connin et al., 1998; Koch et al., 2004).

Throughout the northern Chihuahuan Desert pinyon–juniper–oak woodland (C_3) covered limestone slopes at 1270–1495 m from 42 to 10.8 ka. It was replaced by more xeric oak–juniper woodland (C_3) in the latest Pleistocene/early Holocene, and then in the early–middle Holocene (9–7 ka) by desert grassland (C_4) that gave way to Chihuahuan Desert scrub (a mix of desert shrubs, mostly C_3, and CAM succulents) by about 4.2 ka (Van Devender, 1990, 1995). The pollen and soil carbonate isotopic records for basin floor and alluvial fan environments suggest desert grassland (C_4) during periods of woodland at higher elevations and desert scrub with variable desert grasses from the early to middle Holocene (Monger et al., 1998: Buck and Monger, 1999).

It is clear that there were C_4 grasses in the vegetation mix throughout the Pleistocene and that they increased in importance in the early–middle Holocene. For example, grass pollen in Pleistocene sediments from Pendejo Cave, in Rough Canyon, south-central New Mexico, made up less than 10% of the pollen rain but >15% in Holocene sediments (Gish J. unpublished data quoted in Betancourt et al., 2001). Packrat middens in Rocky Arroyo west of Carlsbad record juniper (shrub) grassland in the early and middle Holocene followed around 4 ka by the appearance of more desert shrubs and succulents. The eastern flanks of the Guadalupe Mountains probably also supported some form of grassland throughout the Holocene (Van Devender, 1990).

The presence of C_4 grasslands in southern New Mexico during the glacial period has been explained in terms of low atmospheric CO_2, which would have favored the photosynthetic pathway of C_4 plants, more effective summer moisture than today due to reduced

maximum temperatures, and/or higher rainfall in the early or late summer (Betancourt et al., 2001). Expansion of C_4 grasslands in the middle Holocene may have been a biotic response to greater summer rainfall in the southwestern USA (e.g., Van Devender, 1995; McAuliffe and Van Devender, 1998).

The above discussion indicates that vegetation at Carlsbad during colder intervals of the last ~164 ka (e.g., OIS 6, 4, 3, and 2) was likely pinyon–juniper–oak forest (C_3) with some C_4 grasses on uplands and C_4 grasslands in adjacent valleys and basins. Glacial to interglacial transitions may have seen more xeric oak–juniper woodland (C_3) and an increase in C_4 grasses. Relatively wetter periods within interglacial warm intervals (e.g., OIS 5 and 1) were probably characterized by desert grasslands (C_4) with some C_3 shrubs such as juniper, and during drier times with less reliable rainfall by desert scrub (largely C_3), interspersed with C_4 grasses and succulents (CAM).

This vegetation history suggests that during glacial and colder intervals of the past the main soil CO_2 signature in waters draining to Carlsbad would have been from C_3 plants with some lesser contribution from sparse C_4 grasses. As the predominant trees in the woodland were probably gymnosperms (pines and junipers), the carbon isotopic signature imparted to soil waters was probably slightly enriched in ^{13}C relative to angiosperm C_3 woodlands (Julio Betancourt personal comm., 2005). This is because gymnosperms produce organic matter with $\delta^{13}C$ about 2‰ higher (mean of -23.0 ± 1.5‰ versus mean of -25.1 ± 1.0‰) than produced by angiosperm C_3 species (Van de Water et al., 2002).

The change to juniper–oak woodland and then desert grassland with some C_3 shrubs must have led to an increase in the $\delta^{13}C$ of soil CO_2 above Carlsbad in the very late glacial and early–middle Holocene. A denser cover of C_4 grasses was one factor responsible for this change. A second factor may have been the effect of warmer and drier conditions on the $\delta^{13}C$ of the woodland trees. Koch et al. (2004) found that leaf $\delta^{13}C$ of C_3 gymnosperms and angiosperms in New Mexico becomes less negative with decreasing elevation. A negative correlation between leaf $\delta^{13}C$ and precipitation suggests that increased moisture stress leads to an increase in leaf $\delta^{13}C$. Thus, the warmer, drier conditions at Carlsbad Cavern at the beginning of the Holocene probably placed tree species under increasing moisture stress possibly resulting in the production of organic matter enriched in ^{13}C.

In the middle and late Holocene the change to desert scrub (largely C_3) and succulents (CAM), with some C_4 grasses, must have produced soil CO_2 depleted in ^{13}C relative to the early Holocene. However, because of the relatively sparse vegetation and small volume of biogenic CO_2 in the soil, atmospheric CO_2 ($\delta^{13}C=-6$ to -8‰) probably played a more important role in carbonate dissolution than during wetter periods, causing ^{13}C enrichment of dissolved species in waters draining into Carlsbad Cavern.

Carlsbad Cavern is presently an extremely dry cave because of the slow percolation of water into it and because it is periodically "freshened" by the influx of cold, dry winter air through the natural entrance. Introduction of drier, outside air with lower pCO_2 increases the rate of CO_2 outgassing from drip waters and leads to the preferential loss of ^{12}C and thus enrichment of the remaining water in ^{13}C. Higher levels of ^{13}C are ultimately passed along to speleothem carbonate. We believe that during wetter glacials the increased flow of water to the cave would have increased the pCO_2 of the cave air and moderated outgassing relative to today. Also, pinyon–juniper–oak woodland around the natural entrance during glacials, rather than the desert scrub, grass, and succulents of today, would have limited the influx of outside air into the cave. As a result enrichment of ^{13}C in drip waters as a result of rapid outgassing of CO_2 would have been greater during interglacials than during glacials of the past.

As mentioned above, because water had to travel a greater distance down the side of the Georgia Giant to reach our coring site as its height increased, there may have been a slight but steady enrichment in both ^{18}O and ^{13}C of the core carbonate over time. We believe that both ^{18}O and ^{13}C were probably enriched more during intervals of drier than wetter climate because of lower humidity and pCO_2 at these times, coupled with reduced drip rates. However, because the relative difference in mass between $^{12}CO_2$ and $^{13}CO_2$ is much less than that between $H_2^{16}O$ and $H_2^{18}O$, C isotopes may be less affected by these kinetic processes than O isotopes.

A complicating factor in any assessment of the impact of kinetic fractionation on O and C isotopes in Georgia Giant carbonate is that we cannot know when the present entrance to the cave was formed. As our speleothem data go back to 164 ka, it is entirely possible that the modern entrance was not in existence at the beginning of speleothem formation. In this event, there would have been little inflow of cold, dry air during winter and the pCO_2 and humidity of the cave air would have been much higher than today. In fact, it is not inconceivable that speleothem carbonate deposited at

this time was deposited in isotopic equilibrium with its precipitating waters.

If the effects listed above are considered together it is possible to assess how and why $\delta^{13}C$ values of carbonate in the Georgia Giant speleothem might have changed over the last 164 ka. During glacial times of cooler and wetter climate, a predominantly C_3 vegetation above the cave would have led to depletion of ^{13}C in percolating waters and in speleothem carbonate. Also, recharge to the limestone would have increased resulting in more rapid flow to the cave allowing less time for exchange of carbon with ^{13}C-rich limestone bedrock. The flow of cool, dry winter air into the cave was probably less than today due to cooler summers and mild winters (Van Devender et al., 1984). An increase in the flow of water to the cave would have increased CO_2 outgassing raising cave air pCO_2. This would have had the feedback effect of reducing the rate of outgassing from later waters entering the cave. Overall, these effects would have limited ^{13}C enrichment of Carlsbad Cavern drip waters and of speleothem carbonate during glacial times.

By contrast, during drier intervals of climate, with conditions similar to those of the early Holocene, percolating waters and speleothem carbonate would be enriched in ^{13}C due to the higher $\delta^{13}C$ of soil CO_2 because of C_4 grasses above the cave, longer residence times in the limestone aquifer before entering cave passages, and more rapid outgassing of CO_2 from drip waters in the cave as a result of the seasonal influx of outside air with low pCO_2.

Based on the above arguments, Georgia Giant carbonate deposited during cold, wet intervals should be depleted in ^{13}C relative to carbonate deposited during warm, dry intervals. However, under climatic conditions similar to today, with a vegetation of desert scrub, succulents, and some C_4 grasses, the $\delta^{13}C$ of speleothem carbonate could be depleted in ^{13}C relative to early-Holocene-age deposits, and even relative to glacial-age deposits because of the relatively high $\delta^{13}C$ of C_3 gymnosperms in the woodland of these times. As pointed out earlier, most desert scrub plants are C_3 and they have a $\delta^{13}C$ of about −25 to −27‰ (Julio Betancourt, personal comm., 2005), compared with C_3 gymnosperms with an average $\delta^{13}C$ of −23‰. However, during the driest periods of the past, when there was C_3 desert scrub vegetation above the cave, there was little or no deposition on the Georgia Giant speleothem because of the extremely dry conditions.

As mentioned earlier, a pure C_3 vegetation will produce stalagmite carbonate ranging in $\delta^{13}C$ from −12 to −8‰, and a pure C_4 vegetation will produce carbonate ranging from −2.3 to +1.5‰ (Cerling, 1984). Values of $\delta^{13}C$ in the Georgia Giant range from −6.6 to +0.9‰ with bimodal values of −5.6 and −3.5‰. Given the possibilities for ^{13}C enrichment of drip waters in Carlsbad Cavern, as outlined above, the range of $\delta^{13}C$ values obtained must be considered a range of maximum values when considering what they might mean about vegetation above the cave.

We believe that ^{13}C enrichment in the Georgia Giant core records periods of warmer, drier climate with predominantly summer rainfall, when the percentage of C_4 grasses in the vegetation above the cave was higher, groundwater flow times from the surface to the cave were longer, and seasonal influxes of dry air into the cave resulted in more evaporation and more rapid outgassing of CO_2—all of which would produce ^{13}C-enriched speleothem carbonate. On the other hand, depleted carbonate in the core may record cool periods with increased moisture largely derived from increased winter precipitation, which supported a largely C_3 woodland above the cave. Increased recharge to the aquifer reduced groundwater flow times to the cave, thus limiting carbon exchange between the bedrock and dissolved species in the water. Finally, cooler summers and wet, mild winters reduced the flow of dry, low pCO_2 air into the cave thus limiting rapid CO_2 outgassing and enrichment of ^{13}C in drip waters.

Very low values of $\delta^{13}C$, around −6‰, occur at about 20–40, 80–150, 238, 300 and 320 cm in the core, or at ~80–105, ~150–165, ~65, 16 and 11 ka. Three of these possible cool moist intervals correlate with glacial OIS 6, 4 and 2, the other with substage 5b, a colder interval during OIS 5. The highest $\delta^{13}C$ values in the record, around −1 to −2‰, occur at 40–75 and ~165 cm or 135–147 and ~110 ka. These possibly warmer and drier intervals correlate with the start of warm OIS 5e and OIS 5c, respectively.

With no ^{13}C enrichment of groundwaters on their way to Carlsbad Cavern, and no enrichment as a result of rapid outgassing of CO_2 once the waters reach the cave, a speleothem carbonate $\delta^{13}C$ of about −6‰ would indicate vegetation above the cave with around 60% C_4 plants and 40% C_3 plants. Likewise, a $\delta^{13}C$ of −2 to −1‰ would indicate vegetation with 100% C_4 plants. There is little doubt that during wet and dry periods of the past, as today, there was enrichment of ^{13}C in Carlsbad Cavern drip waters before speleothem carbonate was precipitated. Therefore, the above estimates of C_4 plants in the vegetation during wet and dry periods are certainly overestimates, although they do suggest significantly more C_3 plants above the cave during glacial than during interglacial intervals.

6. Correlations and comparisons

6.1. Global comparisons

Exact correlation with the SPECMAP record of Imbrie et al. (1984) and Martinson et al. (1987) is difficult because of the large 2σ range of our AS ages, but phases of most rapid growth of the Georgia Giant, as well as phases of low $\delta^{13}C$, appear to correlate with cooler marine isotope stages 6, 4, and 2, and with the cool phases of OIS 5 (OIS 5d and 5b) (Fig. 5). By contrast, the Georgia Giant stopped growing during OIS 5e and 1, and there was only slow growth with abundant aragonite during other warm phases of OIS 5 (5c and 5a). These comparisons suggest that, over the last 164 ka, global warm intervals of the marine oxygen isotope record brought relatively dry conditions to southeastern New Mexico, whereas global cool conditions brought increased wetness. There was also no deposition on the sampled regions of the speleothem during the last 13 ka of OIS 3 and the first 7 ka of OIS 2, suggesting that these intervals may also have been somewhat dry. The broad agreement between the Georgia Giant record and ice cores and ocean cores that reflect global changes in climate suggests that ice sheet fluctuations directly influenced conditions in southern New Mexico.

The Georgia Giant's continuous isotope record from 70 ka to 40 ka also shows striking correlation with distant records (Fig. 6). Higher values of $\delta^{13}C$ in the Georgia Giant are correlative with higher $\delta^{13}C$ values in a stalagmite from Crevice Cave, Missouri (Dorale et al., 1998) and with higher $\delta^{18}O$ values in glacial ice in the GRIP core from Greenland (Dansgaard et al., 1993; Stuiver and Grootes, 2000). As in the longer-term comparison, wetter (lower-$\delta^{13}C$ values) phases at Carlsbad, like those in Missouri, are correlative with cooler intervals in the high-latitude record. These correlations further suggest a strong linkage between ice sheet fluctuations, including Bond cycles and D–O and Heinrich events (Heinrich, 1988), and conditions in southern New Mexico.

Winograd et al. (1992, 1997) contend that in the DH-11 core from Devils Hole, Terminations II and III occur

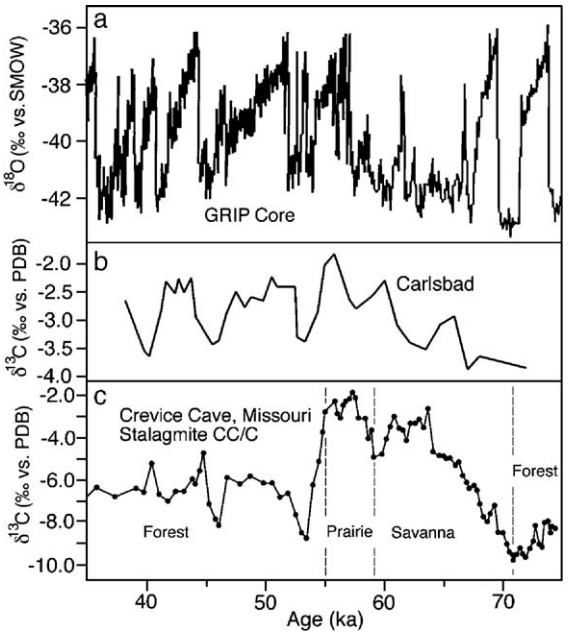

Fig. 6. Comparison of records for the period from 70 to 40 ka. (a) O isotope record from the Greenland Ice Sheet GRIP core (Stuiver and Grootes, 2000); (b) Smoothed three-point running mean C isotope record from Georgia Giant speleothem (samples containing aragonite corrected to 100% calcite equivalent); (c) C isotope record from the Crevice Cave CC/C stalagmite and interpreted vegetation conditions in the area (after Dorale et al., 1998).

at 142±3 and 253±3 ka, whereas in the SPECMAP record these boundaries are at 128±3 and 244±3 ka (Martinson et al., 1987). In the Vostok record Termination II is likewise at 140±15 ka, and the isotope record for Jerusalem West Cave in Israel shows a rapid change in climate at ~140 ka, followed by a brief downturn and then further rapid warming at ~134±5 ka. However, Frumkin et al. (1999) note some disturbance of U in this part of the Jerusalem West stalagmite, adding uncertainty to the TIMS ages (Frumkin et al., 1999). In addition, isotopic and geochemical data from Owens Lake (California) core OL-92 indicate a date for Termination II around 140 ka (Li et al., 2004). Winograd (2002) argues that many AS and TIMS ages for speleothems in NW Europe of 133–115 ka (Baker et al., 1993, 1995), 135–114 ka (Gascoyne, 1981; Gascoyne et al., 1981), and 145–144 ka (Lauritzen,

Fig. 7. The growth record for the Georgia Giant speleothem compared with other climate records for the southwestern United States and northern Mexico. All records are oriented so that wetter conditions are upward. (a) Babicora Basin, Mexico (Metcalfe et al., 2002); (b) Searles Lake (Smith, 1984); (c) Lakes Bonneville and Lahontan (McCoy, 1987; Oviatt et al., 1987; Benson et al., 1990; Morrison, 1991); (d) Browns Room water table elevations (Szabo et al., 1994); (e) Texas Stalagmites (Musgrove et al., 2001); (f) Grand Canyon travertines (Szabo, 1990); (g) this study; (h) Death Valley tufas (Ku et al., 1998); (i) level of Lake Manly (Ku et al., 1998); (j) marine isotope stages (Imbrie et al., 1984; Martinson et al., 1987); (k) $\delta^{18}O$ variations of sulfates from Core DV 93-1, Death Valley, California (Yang et al., 1999); (l) $\delta^{18}O$ of carbonate in Owens Lake core OL-92, California (Menking et al., 1997). The dashed line indicates the overflow threshold of the lake as determined by Bischoff et al. (1997).

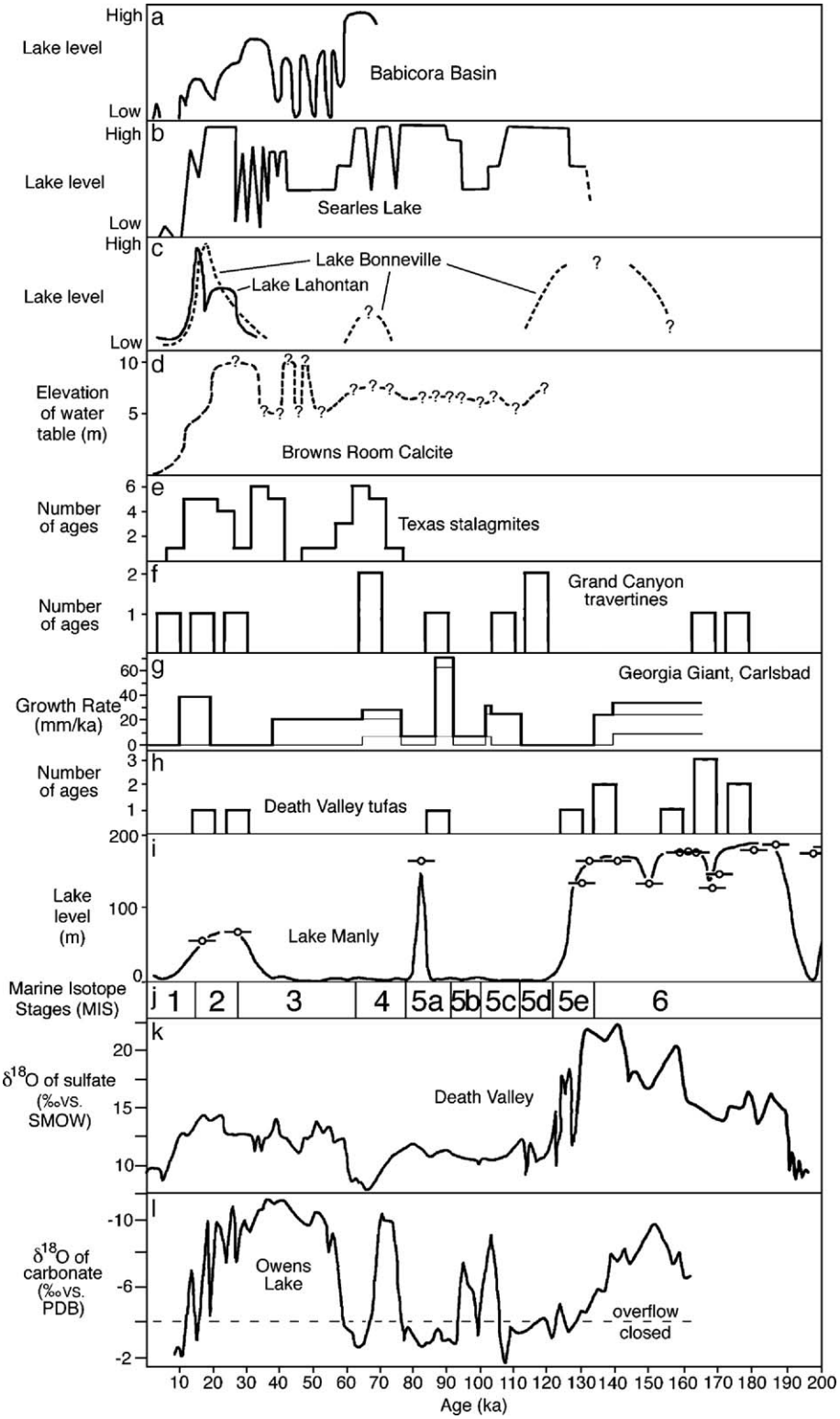
a
High
Lake level
Low
Babicora Basin
b
High
Lake level
Low
Searles Lake
c
High
Lake level
Low
Lake Bonneville
Lake Lahontan
d
10
5
Elevation of water table (m)
Browns Room Calcite
e
6
4
2
Number of ages
Texas stalagmites
f
2
1
Number of ages
Grand Canyon travertines
g
60
40
20
0
Growth Rate (mm/ka)
Georgia Giant, Carlsbad
h
3
2
1
Number of ages
Death Valley tufas
i
200
100
0
Lake level (m)
Lake Manly
Marine Isotope Stages (MIS)
j 1 2 3 4 5a 5b 5c 5d 5e 6
k
20
15
10
δ18O of sulfate (‰vs. SMOW)
Death Valley
l
-10
-6
-2
δ18O of carbonate (‰vs. PDB)
Owens Lake
overflow
closed
10 20 30 40 50 60 70 80 90 100 110 120 130 140 150 160 170 180 190 200
Age (ka)

1995; Berstad et al., 1997) confirm that by 133 ka to possibly by 145 ka the Fennoscandian and British ice sheets had retreated sufficiently for development of biologically active soils, a prerequisite for speleothem growth. Further support for this argument comes from Spötl et al. (2002), who presented evidence from Spannegel Cave in the high Austrian Alps that climate had ameliorated sufficiently there by 135±1.2 ka to allow flowstone deposition following the OIS 6 glaciation. The Georgia Giant core likewise shows a rapid change in climate beginning ~140 ka. The large 2σ errors for ages near 140 ka (averaging 11.2±4 ka for 14 ages in the range 149–134 ka) mean that the Georgia Giant age for Termination II is still within the range of the SPECMAP estimate at 128±3 ka, but the ages are more compatible with a start to Termination II earlier than the SPECMAP estimate.

6.2. Comparison with other Southwest U.S. climate records

The relatively high growth rate of the Georgia Giant from 18 to 10 ka correlates well with other evidence of wet conditions in New Mexico during OIS 2 and 3. These include high levels of Lake King 26–19 ka (Wilkins and Currey, 1997) and Lake Cloverdale 23–21 ka (Krider, 1998), and expanded lakes in the Estancia Basin at 23 and 16 ka (Allen and Anderson, 1993) and in the San Agustin Plains at intervals from 29 to 16 ka (Markgraf et al., 1984; Phillips et al., 1992). They also include speleothem evidence from the Guadalupe Mountains indicating wetter conditions than now during the Younger Dryas from 12.5 to 10.5 ka (Polyak et al., 2004). The lengthy record from the San Agustin Plains of New Mexico indicates high lake levels prior to ~40 ka, dry conditions from 40 to 31 ka, and then a series of high lake levels at 29, 26, 20, and 16 ka followed by drying of the lake basin (Phillips et al., 1992). This record broadly parallels our data from Carlsbad showing increased wetness in southeastern New Mexico prior to 35 ka, drier conditions from 35 to 17 ka, and then wetter conditions from 17 to 11 ka that were followed by conditions as dry as or drier than today.

Variation in growth rate in the Georgia Giant speleothem from Carlsbad also shows a good general agreement with paleoenvironmental records from other southwestern U.S. states and adjacent parts of Mexico (Fig. 7). These include lake records for the Bonneville, Lahontan, Manly, Searles, and Owens basins in the western United States and the Alta Babicora basin in northern Mexico, and frequency of ages of speleothems in three Texas caves and of tufas and travertines in Death Valley and the Grand Canyon. All of these records, including the growth record from the Georgia Giant, indicate that the last few thousand years have been exceptionally dry, a generalization further supported by the observation that many speleothems in Carlsbad have stopped growing and growth rates are slow in formations that are still active (Hill, 1987).

Most of the records from the southwestern US suggest wetter conditions during OIS 2 and 4. Correlations are more difficult in OIS 3 and 5, but almost all the records suggest dry conditions during OIS 5e, as does the absence of growth in the Georgia Giant. All the records extending sufficiently far back in time suggest relatively wet conditions in OIS 6 and, like the growth record of the Georgia Giant, they suggest a more sustained and extensive wet phase in OIS 6 than in either OIS 2 of OIS 4.

All of these lines of evidence taken in combination indicate broadly synchronous climate changes throughout the southwestern U.S. during the last 180 ka. This implies that large-scale atmospheric changes affected the region, the most likely being the northward migration of the polar jet stream during periods of global warmth and its migration south during periods of global cold (see also Benson et al., 2003).

7. O isotopes, paleotemperatures, and atmospheric circulation

7.1. Non-equilibrium considerations

Factors that may have influenced $\delta^{18}O$ of the Georgia Giant include: (i) variations in atmospheric and cave temperatures; (ii) variations in ocean $\delta^{18}O$, which was 1.3 to 1.8‰ higher during glacial maxima; (iii) the source of moisture supplying drip water to the cave; (iv) the inverse relationship with precipitation amount; (v) the dominance of summer versus winter precipitation, the former being enriched in ^{18}O compared to the latter (Nativ and Riggio, 1989, 1990); (vi) the magnitude of kinetic fractionation (evaporation or rapid outgassing of CO_2) of drip water or water films precipitating carbonate (see also McDermott, 2004; Quade, 2004).

The occurrence of some of the lowest $\delta^{18}O$ values in Georgia Giant carbonate from globally cool OIS 6 (Fig. 5) suggests that temperature was not the dominant control on $\delta^{18}O$ values and that the other factors listed above were more important. At present, most rainfall at Carlsbad Cavern is brought by Pacific and Gulf of Mexico maritime tropical air masses during the summer

months. This rainfall appears to affect drip rates in the cave within 1–3 months, but less intense and shorter duration winter rains with lower $\delta^{18}O$ values brought by polar and maritime polar air masses have little effect (personal comm, Paul Burger, Hydrologist, Carlsbad Caverns National Park, 2001).

As precipitation is derived from two very different sources in summer and winter there is a marked seasonal variation in the stable isotope ratios of precipitation. Hoy and Gross (1982) note that mean monthly $\delta^{18}O$ of precipitation at Roswell, NM from 1976 to 1978 ranged from about −13 to −9‰ in the months November to March and from about −6 to 0.0‰ in the months April to October, clearly demonstrating that summer precipitation is enriched in ^{18}O compared with winter precipitation. Ten grab samples of precipitation from Carlsbad from November 1984 to July 1985 also showed a seasonal trend varying from January snow samples with $\delta^{18}O$ of −22.5‰ to a July thunderstorm with $\delta^{18}O$ of −3.1‰ (Chapman, 1986).

Thus, water reaching Carlsbad's passages and rooms has been transported a relatively short distance, has not been affected greatly by 'rainout' of ^{18}O, and therefore has relatively high $\delta^{18}O$ values (−6.0‰ SMOW; Hoy and Gross, 1982). During colder to full glacial conditions, polar and maritime polar air masses, bringing moisture from more northerly and colder ocean locations, may have been more dominant as a result of a more southerly polar jet stream (a possibility considered further below). In such a system, it is likely that atmospheric precipitation was largely in winter and spring. This would have increased the rainout effect on moisture reaching Carlsbad, would have lowered condensation temperatures in the upper atmosphere, and thus would have produced precipitation depleted in ^{18}O. Under the present dry conditions within the cave, waters are not in isotopic equilibrium (Gonzalez and Lohmann, 1988) so that kinetic effects help determine the isotopic characteristics of recent secondary carbonate deposits, generally enriching them in ^{18}O. These considerations suggest that the effect of higher cave temperatures to produce ^{18}O-depleted carbonate on the Georgia Giant during transitions to interglacials (e.g., late OIS 6 (Fig. 7)) was minor compared to the joint effects of ^{18}O-enriched meteoric waters from the Gulf of Mexico, and increased kinetic fractionation of cave waters due to dryness. During colder periods, possibly dominated by winter and spring rainfall from northern Pacific air masses, meteoric waters were depleted in ^{18}O and cave waters were less affected by kinetic fractionation as discussed above. Less kinetic fractionation resulted from higher humidity and elevated pCO_2 in the cave air due to an increased flow of water to the cave and increased outgassing of CO_2 due to higher levels of soil CO_2 above the cave. These conditions led to ^{18}O-depleted carbonate (e.g., early in OIS 6), despite likely lower temperatures in the cave.

7.2. Equilibrium considerations

$\delta^{18}O$ and $\delta^{13}C$ values of Georgia Giant carbonate deposited during relatively warm and dry conditions were probably affected by kinetic fractionation of the precipitating water. As explained previously, the influx of cold, dry, low pCO_2 winter air would have increased evaporation and promoted rapid outgassing of CO_2 from drip waters. However, in the central part of the core from about 70 to 150 cm, calcite accumulated on the top of a growing stalagmite and it is much more likely that carbonate deposited here was in isotopic equilibrium with precipitating waters. Talma and Vogel (1992) have suggested that on flat upper surfaces of stalagmites deposition may be in isotopic equilibrium while kinetic processes affect deposition away from the center as waters flow down the flanks of the stalagmite. From 70–150 cm there is no change in $\delta^{13}C$ despite changes of more than 2‰ in $\delta^{18}O$, which also suggests isotopic equilibrium deposition. It is also possible that when the oldest part of the core was being deposited, more than 140 ka ago, the cave was more closed to the outside than it is today so that the seasonal inflow of dry air may not have been as pronounced. In fact, it is not out of the question that the natural opening through which winter air enters the cave today was not in existence 140 ka ago.

If deposition of the central part of the core was in isotopic equilibrium or very close to it, then isotopic fractionation should have followed the equation of Kim and O'Neil (1997),

$$1000\ln\alpha(\text{calcite}-H_2O) = 18.03(10^3/T)-32.42,$$

which can be transformed to yield ancient water compositions as follows:

$$\delta^{18}O_{water} = [(1000 + \delta^{18}O_{calcite})/(e^{(18.03/T)-0.03242})] - 1000$$

where T is temperature in K and $\delta^{18}O_{calcite}$ and $\delta^{18}O_{water}$ are the oxygen isotopic compositions of the speleothem and precipitating water with respect to SMOW.

Use of the equation above requires estimation of paleotemperature. Noble gas paleotemperatures for ^{14}C-dated groundwaters in New Mexico and Texas were 5.4±0.7 °C lower during the last glacial maximum

(LGM) than during the Holocene, and 2.5 °C lower during the middle Wisconsin 26–39 ka (Stute et al., 1992, 1995). Annual summer and winter temperatures at Potato Lake, Arizona, based on the occurrence of macrofossils of Engelmann spruce, were −4.3, −5.7, and −3.1 °C, respectively, relative to today from 41 to 25 ka, and −5.2, −7.0, and −3.8 °C from 25 to 12 ka (Anderson, 1993). As the present mean annual temperature at Carlsbad is ~16.5 °C and the temperature inside the cave ~14.5 °C, the above data imply a temperature during OIS 6 about 5.5 °C lower than now, or 11 °C above the cave and 9 °C inside it. If Crowley (1994) is correct that OIS 6 was colder than OIS 2, with a more extensive Laurentide Ice Sheet, then actual temperatures may have been even lower.

Our data show that during OIS 6, from 165 to 140 ka, $\delta^{18}O_{calcite}$ varied between −9.5‰ and −7.0‰ PDB (Fig 3). If temperatures in the cave were about 9 °C (or 5.5 °C below present), $\delta^{18}O_{water}$ of drip waters on the Georgia Giant must have been in the range −8.0‰ to −10.5‰ (−8.3‰ to −10.7‰ for an assumed cave temperature of 8 °C and −7.8‰ to −10.3‰ for a cave temperature of 10 °C). Weighted mean $\delta^{18}O$ of recent rainfall and groundwater in the Roswell Basin north of Carlsbad is −6.0‰ (Hoy and Gross, 1982) and it is −6.3‰ at Midland in the southern High Plains of Texas east of Carlsbad (Nativ and Riggio, 1989). This suggests that during OIS 6 rainfall was between 1.7‰ and 4.5‰ lighter than today despite an increase in ocean $\delta^{18}O$ of 1.3 to 1.8‰. Phillips et al. (1986) report that Pleistocene-age groundwaters in the central San Juan Basin of New Mexico average 3‰ lighter than modern groundwater, although several groundwaters studied were 5–6‰ lighter. Dutton (1995) reports unconfined Holocene groundwater in the southern High Plains of Texas ~−6‰, similar to present-day rainfall, and Pleistocene confined waters in the same region ~−10.5‰, a depletion of 4.5‰ (see Fig. 6 of Dutton, 1995). $\delta^{18}O$ of Pleistocene groundwater thus supports our finding that during OIS 6 rainfall was likely depleted by up to 4.5‰ with respect to the modern value. This agreement also implies that noble gas estimates of LGM temperatures, about 5.5 °C below present, are realistic based on the Georgia Giant speleothem data.

7.3. Atmospheric circulation

One possible explanation for ^{18}O-depleted precipitation and groundwater during colder intervals is an increase in moisture from the northern Pacific, as occurs today in winter, relative to the present situation where most moisture comes from the Gulf of Mexico. For this to occur would require the southward displacement of the polar jet stream as a result of the growth of the Laurentide Ice Sheet.

In fact, the southward displacement of westerly storm tracks during the last glaciation is now widely accepted as the primary cause of high lake levels across the southwestern United States and into northern Mexico (Antevs, 1952; Harrison and Metcalfe, 1985; COHMAP members, 1988; Allen and Anderson, 1993; Thompson et al., 1993; Bradbury, 1997; Metcalfe et al., 2002). By contrast, a northward shift in the jet stream during the late glacial has been used to explain the south-to-north shift in the latitude of maximum precipitation during the late Wisconsin with warming of the climate (Phillips et al., 1992). For example, lake stands in the San Agustin Plains of New Mexico at 26, 22, 20, and 16 were progressively lower; whereas lacustrine chronologies for the Great Basin show gradually increasing lake stands until about 16 ka (Benson et al., 1990). Modeling indicates that during the LGM the Laurentide ice sheet caused a split in the jet stream over N. America, especially during the winter months, with one branch displaced to the south across the southern United States and northern Mexico. At this time, the southwestern United States would have been dominated by mid-latitude cyclonic storms most of the year and lower summer temperatures and less thermal energy in the Gulf of Mexico would have hampered the development of convectional storms (Kutzbach and Guetter, 1986; COHMAP members, 1988). Furthermore, a major feature of the ice-age ocean was a warming of the Pacific subtropical gyre, particularly in winter, and a cooling of the Atlantic, particularly in summer. Therefore, because the moisture content of the air overlying the ocean is a strong function of sea-surface temperature, this would produce a wetter ice-age climate in the American southwest, particularly in winter and a somewhat drier climate in summer (Imbrie et al., 1983). Such a scenario would explain depletion of meteoric waters in the Carlsbad region during cold climate events as moisture from the Gulf of Mexico is enriched in ^{18}O relative to moisture from the Pacific as the latter undergoes more rainout of the heavier isotope.

Model simulations show that by 14 ka the jet stream was no longer split and the Westerlies over the southwestern United States were significantly weaker than during the LGM but the south-central United States was still cooler with more effective moisture than today (Kutzbach and Guetter, 1986; COHMAP members, 1988). Mid-latitude cyclones probably still dominated, with convectional and tropical storms of limited

importance. By 10.5 ka the Laurentide ice sheet had retreated sufficiently to limit its influence to far northern parts of North America. There was strong westerly flow during the winter but thermal heating of the continental interior during summer promoted an intensified monsoon circulation and tropical Easterlies with a strong southerly onshore flow in the southwestern United States (Kutzbach and Guetter, 1986; COHMAP members, 1988). Mid-latitude cyclones would have been mostly confined to the winter months when strong westerly flow prevailed, but the region would have been subjected to high intensity convectional storms during the summer half-year as today.

LGM temperatures were probably 5–6 °C cooler than now in the southwest United States and there was probably also an increase in precipitation. Elias and Van Devender (1990) infer greater effective moisture 35–14 ka based on insect assemblages in packrat middens in the Big Bend region of the Chihuahuan Desert, Texas. Many grassland species occurred that are now confined to cooler and moister regions to the north and to higher elevations. Woodland plants at lower elevations coupled with high species richness indicate cooler summers and winters not much colder than today (Van Devender et al., 1984; Van Devender, 1990). Most precipitation was in winter–spring, with only modest amounts in summer because subtropical high pressure cells were very weak. Extension of precipitation into early summer and earlier initiation in the fall of winter frontal systems may account for some warm season moisture and partly explain the widespread presence of C_4 grasses in the vegetation. Biotic records thus suggest an equable climate with mild winters and cool summers (e.g., Wells, 1979; Van Devender, 1990).

The NCAR Community Climate Model Version 1 (CCM 1) simulates significant summer warming as early as 16 ka in the southwest U.S., culminating at 11 ka when simulated July temperatures were warmer than today nearly everywhere in North America despite the continued presence of a substantial ice sheet. By contrast, January temperatures remained lower than present in many regions until the mid to late Holocene. Warmer summer temperatures may have increased monsoon rainfall in late glacial periods despite the prevalence of winter rainfall due to the more southerly route taken by mid-latitude storms. After 14 ka most temperate species were replaced by desert species or by broadly tolerant taxa. Biotic evidence indicates that in the early Holocene winter rainfall was still greater than today but higher summer temperatures led to a modest increase in the strength of the Bermuda High and the summer monsoon, and thus increase in summer rainfall. The middle Holocene witnessed a transition from cool, wet winters to maximum Holocene warmth and summer precipitation dominance. The vegetation of this period apparently was a desert-grassland mixed with some woodland and some Chihuahuan Desert elements. In the late Holocene, Chihuahuan desert scrub became established as the biseasonal rainfall shifted slightly back toward winter (Van Devender, 1990).

8. Conclusions

Variations in the growth of the Georgia Giant speleothem from Carlsbad Cavern, as well as variations in the abundance of aragonite, chalcedony, and Fe-bearing phases, indicate that during the last 164 ka glacial intervals OIS 6, 4, and 2 were much wetter than today. By contrast, during the two warmest periods of the past 164 ka, namely OIS 5e and 1, there was no deposition on either side of the speleothem sampled by our core, pointing to conditions as dry or drier than today. Paleovegetative interpretation of C isotope data from the Georgia Giant supports these inferences.

The 164 ka record from Carlsbad parallels data from many other sites in the southwest USA and northern Mexico, and its correspondence with records from marine sediments and ice cores demonstrates the extent to which ice sheet fluctuations directly influenced conditions in southern New Mexico. Detailed correlation of the Georgia Giant's C isotope record with distant speleothem records and with ice core data further documents the linkage of southwestern climate with global-scale extent of glaciation.

^{18}O-depleted carbonate in the Georgia Giant during OIS 6, at a time when the world's oceans were enriched in ^{18}O, suggests that precipitation during cold intervals was brought largely by Pacific air masses in fall, winter and spring as a result of the southward displacement of the polar jet stream by the growth of the Laurentide Ice Sheet.

The timing of Termination II, which is well defined in the isotopic data, agrees with that obtained from Devils Hole in Nevada, raising the possibility that early warming was widespread in the U.S. southwest region by 145 ka. If correct, this raises questions about the cause of climate warming given the lack of agreement with solar radiation trends at high northern latitudes.

Acknowledgements

This research was funded by a grant from the National Geographic Society. We thank Ron Kerbo then

at Carlsbad Caverns National Park and the National Park Service for permission to drill at the cave. Brooks B. Ellwood drilled the core with the assistance of Mark Earley, a former graduate student at the University of Georgia. We also acknowledge the contribution of Ken Eubanks, a former graduate student of Geology at the University of Georgia, for beginning the work on the Georgia Giant core. We thank Jay Quade and Julio Betancourt for extremely useful comments that helped to improve the manuscript.

References

Allen, B.D., Anderson, R.Y., 1993. Evidence from western North America for rapid shifts in climate during the last glacial maximum. Science 260, 1920–1923.

Anderson, R.S., 1993. A 35,000 year vegetation and climate history from Potato Lake, Mogollon Rim, Arizona. Quaternary Research 40, 351–359.

Antevs, E., 1952. Cenozoic climates of the Great Basin. Geologische Rundschau 40, 94–108.

Baker, A., Smart, P.L., Ford, D.C., 1993. Northwest European palaeoclimate as indicated by growth frequency variations of secondary calcite deposits. Palaeogeography, Palaeoclimatology, Palaeoecology 100, 291–301.

Baker, A., Smart, P.L., Edwards, R.L., 1995. Paleoclimate implications of mass spectrometric dating of a British flowstone. Geology 23, 309–312.

Benson, L.V., Curry, D.R., Dorn, R.I., Lajoie, K.R., Oviatt, C.G., Robinson, S.W., Smith, G.I., Stine, S., 1990. Chronology of expansion and contraction of four Great Basin lake systems during the past 35,000 years. Palaeogeography, Palaeoclimatology, Palaeoecology 78, 241–286.

Benson, L., Lund, S., Negrini, R., Linsley, B., Zic, M., 2003. Response of North American Great Basin Lakes to Dansgaard-Oeschger oscillations. Quaternary Science Reviews 22, 2239–2251.

Berstad, I.M., Einevoll, S., Lauritzen, S.-E., 1997. U-series dating and stable isotope analysis of some last interglacial speleothems from north Norway. Proceedings of the 12th International Congress of Speleology, Symposium, vol. 7, pp. 53–54.

Betancourt, J.L., Rylander, K.A., Peñalba, C., McVickar, J.L., 2001. Late Quaternary vegetation history of Rough Canyon, south-central New Mexico, USA. Palaeogeography, Palaeoclimatology, Palaeoecology 165, 71–95.

Bischoff, J.L., Fitts, J.P., Fitzpatrick, J.A., 1997. Responses of sediment geochemistry to climate change in Owens Lake sediment: an 800 kyr record of saline/fresh cycles. Special Paper-Geological Society of America 317, 37–47.

Boyer, P.S., 1964. Analysis of cave waters from Carlsbad Caverns, New Mexico. Unpublished report on file at Carlsbad Caverns National Park. 58 pp.

Bradbury, J.P., 1997. A diatom record of climate and hydrology for the past 200 ka from Owens Lake, California with comparison to other Great Basin records. Quaternary Science Reviews 16, 203–219.

Brook, G.A., 1999. Arid zone paleoenvironmental records from Cave Speleothems. In: Singhvi, A.K., Derbyshire, E. (Eds.), Paleoenvironmental Reconstruction in Arid Lands. Oxford & IBH, New Delhi, pp. 217–262.

Brook, G.A., Burney, D.A., Cowart, J.B., 1990. Desert paleoenvironmental data from cave speleothems with examples from the Chihuahuan, Somali-Chalbi, and Kalahari Deserts. Palaeogeography, Palaeoclimatology, Palaeoecology 76, 311–329.

Buck, B.J., Monger, H.C., 1999. Stable isotopes and soil geomorphology as indicators of Holocene climate change, northern Chihuahuan Desert. Journal of Arid Environments 43, 357–373.

Cabrol, P., Coudray, J., 1982. Climatic fluctuations influence the genesis and diagenesis of carbonate speleothems in southwestern France. National Speleological Society Bulletin 44, 112–117.

Cerling, T.E., 1984. The stable isotopic composition of modern soil carbonate and its relationship to climate. Earth and Planetary Science Letters 71, 229–240.

Chapman, J.B., 1986. Stable Isotopes in Southeastern New Mexico Groundwater: Implications for Dating Recharge in the WIPP Area. Environmental Evaluation Group Report EEG-35. Environmental Improvement Division, State of New Mexico. 76 pp.

Chapman, J.B., Ingraham, N.L., Hess, J.W., 1992. Isotopic investigation of infiltration and unsaturated zone flow processes at Carlsbad Cavern, New Mexico. Journal of Hydrology 133, 343–363.

COHMAP Members, 1988. Climatic changes of the last 18,000 years: observations and model simulations. Science 241, 1043–1052.

Connin, S.L., Betancourt, J., Quade, J., 1998. Late Pleistocene C4 plant dominance and summer rainfall in the southwestern United States from isotopic study of herbivore teeth. Quaternary Research 50, 179–193.

Crowley, T.J., 1994. Potential reconciliation of Devils Hole and deep-sea Pleistocene chronologies. Palaeoceanography 9 (1), 1–5.

Dansgaard, W., Johnsen, S., Clausen, H.B., Dahl-Jensen, D., Gundestrup, N.S., Hammer, C.U., Hvidberg, C.S., Steffensen, J. P., Sveinbjornsdottir, A.E., Jouzel, J., Bond, G., 1993. Evidence for general instability of past climate from a 250-kyr ice-core record. Nature 364, 218–220.

Dorale, J.A., Edwards, R.L., Ito, E., González, L.A., 1998. Climate and vegetation history of the mid-continent from 75 to 25 ka: a speleothem record from Crevice Cave, Missouri, USA. Science 282, 1871–1874.

Dutton, A.R., 1995. Groundwater isotopic evidence for paleorecharge in U.S. High Plains aquifers. Quaternary Research 43, 221–231.

Edwards, R.L., Gallup, C.D., 1993. Dating of the Devils Hole calcite vein. Science 259, 1626–1627.

Elias, S.A., Van Devender, T.R., 1990. Fossil insect evidence for late Quaternary climatic change in the Big Bend region, Chihuahuan Desert, Texas. Quaternary Research 34, 249–261.

Ellwood, B.B., Balsam, W., Burkart, B., Long, G.J., Buhl, M.L., 1986. Anomalous magnetic properties in rocks containing the mineral siderite: paleomagnetic implications. Journal of Geophysical Research 91, 12,779–12,790.

Ellwood, B.B., Hrouda, F., Wagner, J.J., 1988. Symposia on magnetic fabrics. Physics of the Earth and Planetary Interiors 51 (4), 249–392.

Ellwood, B.B., Burkart, B., Rajeshwar, K., Darwin, R.L., Neeley, R. A., McCall, A.B., Long, G.J., Buhl, M.L., Hickcox, C.W., 1989. Are the iron carbonate minerals, ankerite and ferroan dolomite, like siderite, important in paleomagnetism? Journal of Geophysical Research 94, 7321–7331.

Forbes, J.R., 2000. Geochemistry of Carlsbad Cavern pool waters, Guadalupe Mountains, New Mexico. Journal of Cave and Karst Studies 62 (2), 127–134.

Frumkin, A., Ford, D.C., Schwarcz, H.P., 1999. Continental oxygen isotope record of the last 170,000 years in Jerusalem. Quaternary Research 51, 317–327.

Gascoyne, M., 1981. A climate record of the Yorkshire Dales for the last 300,000 years. Proceedings of the 8th International Congress of Speleology, vol. 1, pp. 96–98.

Gascoyne, M., Currant, A.P., Lord, T.C., 1981. Ipswichian fauna of Victoria Cave and the marine paleoclimate record. Nature 294, 652–654.

Gonzalez, L.A., Lohmann, K.C., 1988. Controls on mineralogy and composition of spelean carbonates: Carlsbad Caverns, New Mexico. In: James, N.P., Choquette, P.W. (Eds.), Paloeokarst. Springer-Verlag, New York, pp. 81–101.

Grossman, E.L., Ku, T.-L., 1986. Oxygen and carbon isotope fractionation in biogenic aragonite: temperature effects. Chemical Geology 59, 59–74.

Harrison, S.P., Metcalfe, S.E., 1985. Spatial variations in lake levels since the last glacial maximum in the Americas north of the equator. Zeitschrift fûr Gletscherkûnde und Glazialgeologie 21, 1–15.

Heinrich, H., 1988. Origin and consequences of cyclic ice rafting in the Northeast Atlantic Ocean during the past 130,000 years. Quaternary Research 29, 142–152.

Hendy, C.H., 1971. The isotopic geochemistry of speleothems I: the calculation of the effects of different modes of formation on the isotopic composition of speleothems and their applicability as palaeoclimatic indicators. Geochimica et Cosmochimica Acta 35, 801–824.

Hill, C.A., 1987. Geology of Carlsbad Cavern and other caves in the Guadaloupe Mountains, New Mexico and Texas. Bulletin-New Mexico Bureau of Mines & Mineral Resources 117. 150 pp.

Hoy, R.N., Gross, G.F., 1982. A baseline study of oxygen 18 and Deuterium in the Roswell, New Mexico, Groundwater Basin. New Mexico Water Resources Research Institute Report 144. 95 pp.

Imbrie, J., McIntyre, A., Moore Jr., T.C., 1983. The ocean around North America at the last glacial maximum. Chapter 12. In: Wright Jr., H. E., Porter, S.C. (Eds.), Late Quaternary Environments of the United States. The Late Pleistocene, vol. 1. University of Minnesota Press, Minneapolis, pp. 230–236.

Imbrie, J., Hays, J.D., Martinson, D., McIntyre, A., Mix, A., Morley, J., Pisias, N., Prell, W., Shackleton, N.J., 1984. The orbital theory of Pleistocene climate: support from a revised chronology of the marine $\delta^{18}O$ record. In: Berger, A.L., et al. (Ed.), Milankovitch and Climate, Part I. D. Reidel, pp. 269–305.

Ingraham, N.L., Chapman, J.B., Hess, J.W., 1990. Stable isotopes in cave pool systems: Carlsbad Cavern, New Mexico, U.S.A. Chemical Geology. Isotope Geoscience Section 86, 65–74.

Jouzel, J., Lorius, C., Petit, J.R., Genthon, C., Barkov, N.I., Kotlyakov, V.M., Petrov, V.N., 1987. Vostok ice core: a continuous isotope temperature record over the last climatic cycle (160,000 years). Nature 329, 403–408.

Kim, S.-T., O'Neil, J.R., 1997. Equilibrium and nonequilibrium oxygen isotope effects in synthetic carbonates. Geochimica et Cosmochimica Acta 61, 3461–3475.

Kitano, Y., Oomori, T., 1971. The coprecipitation of uranium with calcium carbonate. Journal of the Oceanographic Society of Japan 27, 34–43.

Koch, P.L., Diffenbaugh, N.S., Hoppe, K.A., 2004. The effects of late Quaternary climate and pCO_2 change on C_4 plant abundance in the south-central United States. Palaeogeography, Palaeoclimatology, Palaeoecology 207, 331–357.

Krider, P.R., 1998. Paleoclimatic significance of late Quaternary lacustrine and alluvial stratigraphy, Animas Valley, New Mexico. Quaternary Research 50, 283–289.

Ku, T.-L., Luo, S., Lowenstein, T.K., Li, J., Spencer, R.J., 1998. U-series chronology of lacustrine deposits in Death Valley, California. Quaternary Research 50, 261–275.

Kutzbach, J.E., Guetter, P.J., 1986. The influence of changing orbital parameters and surface boundary conditions on climate simulations for the past 18,000 years. Journal of the Atmospheric Sciences 43, 1726–1759.

Lauritzen, S.-E., 1995. High resolution paleotemperature proxy record for the last interglaciation based on Norwegian speleothems. Quaternary Research 43, 133–146.

Li, H.-C., Bischoff, J.L., Ku, T.-L., Zhu, Z.-Y., 2004. Climate and hydrology of the Last Interglaciation (MIS 5) in Owens Basin, California: isotopic and geochemical evidence from core OL-92. Quaternary Science Reviews 23, 49–63.

Markgraf, V., Bradbury, J.P., Forester, R.M., Singh, G., Sternberg, R.S., 1984. San Agustin plains, New Mexico: age and paleoenvironmental potential reassessed. Quaternary Research 22, 336–343.

Martinson, D.G., Pisias, N.G., Hays, J.D., Imbrie, J., Moore, T.C., Shackleton, N.J., 1987. Age dating and the orbital theory of the ice ages: development of a high-resolution 0 to 300,000 year chronostratigraphy. Quaternary Research 27, 1–29.

McAuliffe, J.R., Van Devender, T.R., 1998. A 22,000-year record of vegetation change in the north–central Sonoran Desert. Palaeogeography, Palaeoclimatology, Palaeoecology 141, 253–275.

McConnell, J.B., Busenberg, E., Plummer, L.N., 1994. Water-resources data for the Valdosta area, south-central Georgia 1961–93. USGS Open File Report, pp. 94–350. 58 pp.

McCoy, W.D., 1987. Quaternary aminostratigraphy of the Bonneville basin, western United States. Geological Society of America Bulletin 98, 99–112.

McCrea, J.M., 1950. On the isotopic chemistry of carbonates and a paleotemperature scale. Journal of Chemical Physics 18, 849–857.

McDermott, F., 2004. Palaeo-climate reconstruction from stable isotope variations in speleothems: a review. Quaternary Science Reviews 23, 901–918.

McLean, J.S., 1971. The Microclimate in Carlsbad Caverns, New Mexico. USGS Open File Report, pp. 71–198. 67 pp.

McLean, J.S., 1976. Factors Altering the Microclimate in Carlsbad Caverns, New Mexico. USGS Open File Report, pp. 76–171. 55 pp.

Meece, D.E., Benninger, L.K., 1993. The coprecipitation of Pu and other radionuclides with $CaCO_3$. Geochimica et Cosmochimica Acta 57, 1447–1458.

Menking, K.M., Bischoff, J.L., Fitzpatrick, J.A., Burdette, J.W., Rye, R.O., 1997. Climatic/hydrologic oscillations since 155,000 yr B.P. at Owens Lake, California, reflected in abundance and stable isotope composition of sediment carbonate. Quaternary Research 48, 58–68.

Metcalfe, S., Say, A., Black, S., McCulloch, R., O'Hara, S., 2002. Wet conditions during the last glaciation in the Chihuahuan Desert, Alta Babicora Basin, Mexico. Quaternary Research 57, 91–101.

Monger, H.C., Cole, D.R., Gish, J.W., Giordano, T.H., 1998. Stable carbon and oxygen isotopes in Quaternary soil carbonates as indicators of ecogeomorphic changes in the northern Chihuahuan Desert, USA. Geoderma 82, 137–172.

Morrison, R.B., 1991. Quaternary stratigraphic, hydrologic, and climatic history of the Great Basin, with emphasis on Lakes Lahontan, Bonneville, and Tecopa. In: R.B. Morrison (Ed.),

Quaternary Nonglacial Geology: Conterminous U.S., pp. 283-320. The Geology of North America, K-2, Geological Society of America, Boulder, CO.

Murray, J.W., 1954. The deposition of calcite and aragonite in caves. Journal of Geology 62, 481–492.

Musgrove, M., Banner, J.L., Mack, L., James, E.W., Cheng, H., Edwards, L.R., 2001. Geochronology of the late Pleistocene to Holocene speleothems from central Texas: implications for regional paleoclimate. Geological Society of America Bulletin 113 (12), 1532–1543.

Nativ, R., Riggio, R., 1989. Meteorologic and isotopic characteristics of precipitation events with implications for groundwater recharge, southern High Plains. Atmospheric Research 23, 51–82.

Nativ, R., Riggio, R., 1990. Precipitation in the southern High Plains: meteorologic and isotopic features. Journal of Geophysical Research 95 (D13), 22,559–22,564.

Oviatt, C.G., McCoy, W.D., Reider, R.G., 1987. Evidence for a shallow early or middle Wisconsin-age lake in the Bonneville Basin, Utah. Quaternary Research 27, 248–262.

Phillips, F.M., Peeters, L.A., Tansey, M.K., 1986. Paleoclimatic inferences from an isotopic investigation of groundwater in the central San Juan Basin, New Mexico. Quaternary Research 26, 179–193.

Phillips, F.M., Campbell, A.R., Kruger, C., Johnson, P., Roberts, R., Keyes, E., 1992. A reconstruction of the response of the water balance in western United States lake basins to climate change. New Mexico Water Resources Research Institute Report No. 269, vol. I.

Pobeguin, Th., 1965. Sur les concretions calcaires Observées dans la Grotte de Moulis (Ariège). Société Géologique de la France, Compte Rendu 241, 1791–1793.

Polyak, V.J., Asmerom, Y., 2001. Late Holocene climate and cultural changes in the southwestern United States. Science 294, 148–151.

Polyak, V.J., Rasmussen, J.B.T., Asmerom, Y., 2004. Prolonged wet period in the southwestern United States through the Younger Dryas. Geology 32, 5–8.

Quade, J., 2004. Isotopic records from ground-water and cave speleothem calcite in North America. In: Gillespie, A., Porter, S. C., Atwater, B.F. (Eds.), Developments in Quaternary Science, vol. 1. Elsevier Science, New York, pp. 205–219.

Railsback, L.B., 2000. An Atlas of Speleothem Microfabrics: http://www.gly.uga.edu/speleoatlas/SAIndex1.html.

Railsback, L.B., Brook, G.A., Chen, J., Kalin, R., Fleischer, C.J., 1994. Environmental controls on the petrology of a Late Holocene spleothem from Botswana with annual layers of aragonite and calcite. Journal of Sedimentary Research A64, 147–155.

Romanek, C.S., Grossman, E.L., Morse, J.W., 1992. Carbon isotopic fractionation in synthetic aragonite and calcite: effects of temperature and precipitation. Geochimica et Cosmochimica Acta 56, 419–430.

Siegel, F.R., 1965. Aspects of calcium carbonate deposition in Great Onyx Cave, Kentucky. Sedimentology 4, 285–299.

Siegel, F.R., Dort Jr., W., 1966. Calcite-aragonite speleothems from a hand-dug cave in northeast Kansas. International Journal of Speleology 2, 165–169.

Smith, G.I., 1984. Paleohydrologic regimes in the southwestern Great Basin 0–3.2 myr ago, compared with other long records of "global" climate. Quaternary Research 22, 1–17.

Spötl, C., Mangini, A., Frank, N., Eichstädter, R., Burns, S., 2002. Start of the last interglacial period at 135 ka: evidence from a high Alpine speleothem. Geology 30 (9), 815–818.

Stuiver, M., Grootes, P.M., 2000. GISP2 oxygen isotope ratios. Quaternary Research 53, 277–284.

Stute, M., Schlosser, P., Clark, J.F., Broecker, W.S., 1992. Paleotemperatures in the southwestern United States derived from noble gases in ground water. Science 256, 1000–1003.

Stute, M., Clark, J.F., Schlosser, P., Broecker, W.S., 1995. A 30,000 yr continental paleotemperature record derived from noble gases dissolved in groundwater from the San Juan Basin, New Mexico. Quaternary Research 43, 209–220.

Swartzendruber, L.J., 1992. Properties, units and constants in magnetism. Journal of Magnetic Materials 100, 573–575.

Szabo, B.J., 1990. Ages of travertine deposits in eastern Grand Canyon National Park, Arizona. Quaternary Research 34, 24–32.

Szabo, B.J., Kolesar, P.T., Riggs, A.C., Wingrad, I.J., Ludwig, K.R., 1994. Paleoclimatic fluctuations from a 120,000-yr calcite record of water table fluctuations in Browns Room of Devils Hole, Nevada. Quaternary Research 41, 59–69.

Talma, A.S., Vogel, J.C., 1992. Late Quaternary paleotemperatures derived from a speleothem from Cango Caves, Cape Province, South Africa. Quaternary Research 37, 203–213.

Thompson, R.S., Whitlock, C., Bartlein, P.J., Harrison, S.P., Spaulding, W.G., 1993. Climatic changes in the western United States since 18,000 yr B.P. In: WrightJr. Jr., H.E., et al. (Ed.), Global Climates Since the Last Glacial Maximum. University of Minnesota Press, Minneapolis.

Thrailkill, J., 1971. Carbonate deposition in Carlsbad Caverns. Journal of Geology 79, 683–695.

Van Devender, T.R., 1990. Late Quaternary Vegetation and Climate of the Chihuahuan Desert, United States and Mexico. In: Betancourt, J.L., Van Devender, T.R., Martin, P.R. (Eds.), Packrat Middens: The Last 40,000 Years of Biotic Change. The University of Arizona Press, Tucson, AZ, pp. 104–133. Chapter 7.

Van Devender, T.R., 1995. Desert grassland history: biogeography and community dynamics. In: McClaran, M., Van Devender, T.R. (Eds.), The Desert Grassland. The University of Arizona Press, Tucson, AZ, pp. 68–99.

Van Devender, T.R., Spaulding, W.G., Phillips II, A.M., 1978. Late Pleistocene plant communities in the Guadalupe Mountains Culberson County, Texas. In: Genoways, H.H., Baker, R.J. (Eds.), Biological Investigations in the Guadalupe Mountains National Park, Texas. National Park Service, Washington, DC, pp. 13–30.

Van Devender, T.R., Betancourt, J.L., Wimberley, M., 1984. Biogeographic implications of a Packrat midden sequence from the Sacramento Mountains, south-central New Mexico. Quaternary Research 22, 344–360.

Van de Water, P.K., Leavitt, S.W., Betancourt, J.L., 2002. Leaf $\delta^{13}C$ variability with elevation, slope aspect, and precipitation in the southwest United States. Oecologia 132, 332–343.

Wells, P.V., 1979. An equable glaciopluvial in the west: pleniglacial evidence of increased precipitation on a gradient from the Great Basin to the Sonoran and Chihuahuan deserts. Quaternary Research 12, 311–325.

Wilkins, D.E., Currey, D.R., 1997. Timing and extent of late Quaternary paleolakes in the Trans-Pecos closed basin, west Texas and south-central New Mexico. Quaternary Research 47, 306–315.

Williams, P.W., 1983. The role of the subcutaneous zone in karst hydrology. Journal of Hydrology 61, 45–67.

Winograd, I.J., 2002. Letters to the editor: evidence from uranium-series-dated speleothems for the timing of the penultimate

deglaciation of northwestern Europe. Quaternary Research 58, 60–61.

Winograd, I.J., Szabo, B.J., Coplen, T.B., Riggs, A.C., 1988. A 250,000-year climatic record from Great Basin vein calcite: implications for Milankovitch theory. Science 242, 1275–1281.

Winograd, I.J., Coplen, T.B., Landwehr, J.M., Riggs, A.C., Ludwig, K. R., Szabo, B.J., Kolesar, P.T., Revesz, K.M., 1992. Continuous 500,000-year climate record from vein calcite in Devils Hole, Nevada. Science 258, 255–260.

Winograd, I.J., Landwehr, J.M., Ludwig, K.R., Coplen, T.B., Riggs, A. C., 1997. Duration and structure of the past four interglaciations. Quaternary Research 48, 141–154.

Yang, W., Krouse, H.R., Spencer, R.J., Lowenstein, T.K., Hutcheon, I. E., Ku, T.-L., Li, J., Roberts, S.M., Brown, C.B., 1999. A 200,000-year record of change in oxygen isotope composition of sulfate in a saline sediment core, Death Valley, California. Quaternary Research 51, 148–157.